







The $\text{exo-}\beta\text{-N}$ -acetylmuramidase NamZ from *Bacillus subtilis* is the founding member of a family of exo-lytic peptidoglycan hexosaminidases

Received for publication, January 7, 2021, and in revised form, February 27, 2021. Published, Papers in Press, March 5, 2021.

<https://doi.org/10.1016/j.jbc.2021.100519>

Maraiké Müller¹, Matthew Calvert^{2,3,4}, Isabel Hottmann¹, Robert Maria Kluj¹, Tim Teufel¹, Katja Balbuchta¹, Alicia Engelbrecht¹, Khaled A. Selim^{1,5} , Qingping Xu⁶, Marina Borisova¹ , Alexander Titz^{2,3,4} , and Christoph Mayer^{1,*} 

From the ¹Interfaculty Institute of Microbiology and Infection Medicine, University of Tübingen, Tübingen, Germany; ²Chemical Biology of Carbohydrates, Helmholtz Institute for Pharmaceutical Research Saarland (HIPS), Helmholtz Centre for Infection Research (HZI), Saarbrücken, Germany; ³Deutsches Zentrum für Infektionsforschung (DZIF), Standort Hannover-Braunschweig, Germany; ⁴Department of Chemistry, Saarland University, Saarbrücken, Germany; ⁵Chemistry of Natural and Microbial Products Department, Pharmaceutical and Drug Industries Research Division, National Research Center, Giza, Egypt; and ⁶GM/CA @ APS, Argonne National Laboratory, Lemont, Illinois, USA

Edited by Chris Whitfield

Endo- $\beta\text{-N}$ -acetylmuramidases, commonly known as lysozymes, are well-characterized antimicrobial enzymes that catalyze an endo-lytic cleavage of peptidoglycan; *i.e.*, they hydrolyze the $\beta\text{-1,4}$ -glycosidic bonds connecting *N*-acetylmuramic acid (MurNAc) and *N*-acetylglucosamine (GlcNAc). In contrast, little is known about $\text{exo-}\beta\text{-N}$ -acetylmuramidases, which catalyze an exo-lytic cleavage of $\beta\text{-1,4}$ -MurNAc entities from the non-reducing ends of peptidoglycan chains. Such an enzyme was identified earlier in the bacterium *Bacillus subtilis*, but the corresponding gene has remained unknown so far. We now report that *ybbC* of *B. subtilis*, renamed *namZ*, encodes the reported $\text{exo-}\beta\text{-N}$ -acetylmuramidase. A ΔnamZ mutant accumulated specific cell wall fragments and showed growth defects under starvation conditions, indicating a role of NamZ in cell wall turnover and recycling. Recombinant NamZ protein specifically hydrolyzed the artificial substrate para-nitrophenyl β -MurNAc and the peptidoglycan-derived disaccharide MurNAc- $\beta\text{-1,4}$ -GlcNAc. Together with the $\text{exo-}\beta\text{-N}$ -acetylglucosaminidase NagZ and the exo- muramoyl-L-alanine amidase AmiE, NamZ degraded intact peptidoglycan by sequential hydrolysis from the non-reducing ends. A structure model of NamZ, built on the basis of two crystal structures of putative orthologs from *Bacteroides fragilis*, revealed a two-domain structure including a Rossmann-fold-like domain that constitutes a unique glycosidase fold. Thus, NamZ, a member of the DUF1343 protein family of unknown function, is now classified as the founding member of a new family of glycosidases (CAZy GH171; www.cazy.org/GH171.html). NamZ-like peptidoglycan hexosaminidases are mainly present in the phylum Bacteroidetes and less frequently found in individual genomes within Firmicutes (Bacilli, Clostridia), Actinobacteria, and γ -proteobacteria.

The enzymatic degradation of carbohydrate polymers (glycans) in nature is generally mediated by endo- and exo-lytic glycosidases, which may act synergistically (1–3). Endo-glycosidases bind to an internal site of a glycan and cleave these internal glycosidic bonds (endo-lytic cleavage), thereby solubilizing the polymer and providing oligomeric substrates for exo- glycosidases, which bind to one end of a glycan, mostly the nonreducing end but in rare cases also the reducing end, and chip off monomeric carbohydrates or disaccharides (exo-lytic cleavage) (2, 4). Accordingly, cellulose (poly- $\beta\text{-1,4}$ -glucose), the main glycan component of plants, and chitin (poly- $\beta\text{-1,4-N}$ -acetylglucosamine), the main glycan component of fungi and arthropods, are degraded by various organisms involving complex sets of lytic enzymes. These include endo-lytic glycanases (endo-cellulases or endo-chitinases, respectively) and exo-lytic glycanases, (cellobiohydrolases and diacetylchitobiohydrolases, respectively) as well as exo-lytic glycosidases (β -glucosidases/cellobiases and $\beta\text{-N}$ -acetylglucosaminidases/diacetylchitobiases, respectively) (2, 4).

Considerably less is known about the synergistic cooperation of endo- and exo-lytic enzymes degrading peptidoglycan, the cell wall heteropolymer of bacteria. Peptidoglycan is composed of polysaccharide chains of alternating $\beta\text{-1,4}$ -linked *N*-acetylglucosamine (GlcNAc) and *N*-acetylmuramic acid (MurNAc) carbohydrates that are interweaved forming a network *via* short oligopeptides linked to the 3-O-lactoyl residues of MurNAc (5). Despite the general lack of knowledge about synergistic peptidoglycan degradation, endo-muramidases catalyzing endo-lytic cleavage of the MurNAc- $\beta\text{-1,4}$ -GlcNAc bond belong to the class of the best studied enzymes, notably hen's egg white lysozyme, representing prominent antimicrobial defense molecules (6, 7). Most knowledge about peptidoglycan decomposition, however, relates to a bacterial metabolic process known as peptidoglycan turnover and recycling (8–10). During growth, bacteria need to degrade their own peptidoglycan to allow cell expansion, cell

* For correspondence: Christoph Mayer, christoph.mayer@uni-tuebingen.de. Present address for Matthew Calvert: Department of Chemistry, University of Auckland, Auckland, New Zealand.

Exo-muramidase NamZ of *B. subtilis*

division, and daughter cell separation. Besides endopeptidases and amidases that target the peptide part of the peptidoglycan, the process of peptidoglycan turnover involves endo-lytic glycosidases that cleave either of the two glycosidic bonds within the peptidoglycan backbone: the MurNAc- β -1,4-GlcNAc-linkage (endo- β -*N*-acetylmuramidases; e.g., lysozymes) or the GlcNAc- β -1,4-MurNAc-linkage (endo- β -*N*-acetylglucosaminidases). The former enzymes include lysozyme-like muramidases, which catalyze a hydrolytic cleavage, and also a special type of muramidases, called lytic transglycosylases, which catalyze nonhydrolytic cleavage of the same bond, releasing products containing a 1,6-anhydroglycosidic form of MurNAc (anhMurNAc) via an intramolecular transglycosylation reaction (11, 12). The latter enzymes are known as peptidoglycan-hydrolysing endo- β -*N*-acetylglucosaminidases (e.g., Atl^{Glc} or SagB of *Staphylococcus aureus*; (13–15)). Whereas endo- β -*N*-acetylmuramidases and lytic transglycosylases generate oligosaccharides carrying a GlcNAc at the nonreducing end, endo- β -*N*-acetylglucosaminidases produce glycans with a MurNAc at the nonreducing end. Peptidoglycan fragments carrying a GlcNAc at the nonreducing end are further processed by exo-lytic β -*N*-acetylglucosaminidases (exo-GlcNAc^{ases}), which cleave off terminal, nonreducing GlcNAc residues. These ubiquitous enzymes are classified into different families of glycosidases (CAZy glycosidase families 3, 20, 84) (<https://www.cazy.org>). Many of them have been biochemically and mechanistically characterized in great detail, e.g., β -*N*-acetylglucosaminidases belonging to family 3 of glycosidases, such as NagZ of *Bacillus subtilis*, *Escherichia coli*, and *Pseudomonas aeruginosa*, are well-known enzymes of the bacterial cell wall recycling pathways (16–18). In contrast, almost nothing is known about exo-lytic β -*N*-acetylmuramidases, which cleave terminal, nonreducing MurNAc residues that occur in peptidoglycan fragments generated by endo- β -*N*-acetylglucosaminidases. The only reports of an enzyme with exo- β -*N*-acetylmuramidase activity come from Del Rio and co-workers (19, 20). They identified such an enzyme entity that occurs partly in the medium and partly bound to cells of *B. subtilis* at the end of exponential growth and biochemically characterized the purified enzyme (19, 20). The encoding gene, however, has remained unknown, so far. We are investigating the function of peptidoglycan recycling and MurNAc catabolic operon of *B. subtilis* 168 (*murQ-murR-murP-amiE-nagZ-ybbC*) (16, 21). This operon consists of genes required for MurNAc catabolism: *murQ*, encoding a cytoplasmic MurNAc 6-phosphate (MurNAc-6P) lactyl ether hydrolase (22), *murR*, encoding a MurNAc-6P-sensing transcriptional regulator (23), and *murP*, encoding a MurNAc-specific phosphotransferase type transporter (24). Further, the operon contains *amiE* and *nagZ*, encoding two secreted exo-acting hydrolases, the exo-muramoyl-L-alanine amidase AmiE and the exo- β -*N*-acetylglucosaminidase NagZ, which are required for muropeptide rescue in *B. subtilis*, as shown earlier by our group (8, 16). We report here the identification of *ybbC*, the last gene within this operon, to encode the secreted exo-*N*-acetylmuramidase of *B. subtilis* 168. The enzyme, referred to as NamZ hereafter,

was biochemically characterized using the chromogenic substrate para-nitrophenyl 2-acetamido-3-O-(D-1-carboxyethyl)-2-deoxy- β -D-glucopyranoside (pNP-MurNAc) and the natural, peptidoglycan-derived disaccharide MurNAc-GlcNAc. NamZ specifically hydrolyzed pNP-MurNAc, MurNAc-GlcNAc and peptidoglycan fragments carrying a β -1,4-MurNAc entity at the nonreducing end, whereas the NagZ substrates pNP-GlcNAc, GlcNAc-MurNAc and peptidoglycan fragments carrying a β -1,4-GlcNAc entity at the non-reducing end are not hydrolyzed by NamZ. Together with two further secreted enzymes, the exo-muramoyl-L-alanine amidase AmiE and the exo-*N*-acetylglucosaminidase NagZ of *B. subtilis*, NamZ cleaves peptidoglycan and fragments thereof (muropeptides), sequentially from the nonreducing end, thereby releasing MurNAc, GlcNAc, and peptidoglycan peptides, which can be taken up by the cell and further metabolized in the cytoplasm (16, 21). Thus, in contrast to the degradative systems of the homopolymers cellulose and chitin, the cleavage of the heteropolymer peptidoglycan involves two distinct sets of exo- and endo-lytic β -hexosaminidases: exo- and endo-acting β -*N*-acetylglucosaminidases as well as exo- and endo-acting β -*N*-acetylmuramidases. Here we propose that NamZ of *B. subtilis* is the founding member of a unique family of exo-lytic β -*N*-acetylmuramidases, which is mainly present in the phylum of *Bacterioidetes* and, less frequently, within *Bacilli*, *Clostridia*, *Actinobacteria*, and γ -*proteobacteria*.

Results

The *B. subtilis* *ybbC* (*namZ*) mutant displays defects in cell growth and exo- β -*N*-acetylmuramidase function

The function of *ybbC*, the last gene within the peptidoglycan/MurNAc recycling operon of *B. subtilis* 168 (*murQ-murR-murP-amiE-nagZ-ybbC*), remained unknown so far (16, 21). It encodes a putative enzyme with no significant sequence identity toward any protein of known function, containing a conserved protein domain of unknown function (PFAM DUF1343 or PF07075). The location of *ybbC* in an operon next to *nagZ* and transcriptional analyses of *B. subtilis* cells grown under different conditions indicated that the expression of both genes is coregulated and, thus, suggested a related function (16, 25). We hypothesized that *ybbC* may encode the enigmatic, secreted exo- β -*N*-acetylmuramidase, identified by Del Rio *et al.*, and functioning in conjunction with NagZ (16, 19, 20). A putative signal peptide motif (MRKTI-FAFLTGLMMFGTITAASA/SPD;/, cleavage site according to signal P-5.0 (26)) suggested that the *ybbC*-encoded protein is secreted. To obtain a first indication that *ybbC* encodes the unknown exo- β -*N*-acetylmuramidase coregulated with NagZ, termed NamZ, we compared growth and extracellular accumulation of cell wall fragments in rich medium (LB) of *B. subtilis* 168 (wild-type; WT), Δ *nagZ*, and Δ *namZ* (Δ *nagZ::erm* and Δ *namZ::erm* obtained from the *Bacillus* Genetic Stock Center (27) were rendered markerless by excision of the erythromycin resistance cassettes, as described in the [Experimental procedures](#)). We observed that the two mutants showed a similar behavior by OD measurements during

growth, which differed from that of the WT, in that the two mutants reached lower OD₆₀₀ values in early stationary phase compared with the WT strain (Fig. S1). This is consistent with the reported expression profile of *nagZ*, in which protein levels were very low during the exponential phase, but strongly increased during transition and stationary phase (16). However, following prolonged stationary phase (52 h of growth; Fig. S1), both the $\Delta namZ$ and the $\Delta nagZ$ mutant displayed a diminished lytic phenotype compared with WT, as reported earlier for *nagZ* (16).

A mass spectrometric analysis of the supernatants of mutants and WT cells was conducted to identify the cell wall fragments that specifically accumulated in the supernatants of $\Delta namZ$ and $\Delta nagZ$ and may indicate the absence of exo-muramidase function in the *namZ* deficient strain. As expected, no significant accumulation of small soluble products was observed in the supernatants of exponentially growing cells (5 h; data not shown). Further, the analysis of stationary phase supernatants (20 h) also revealed only minor differences in the accumulation of small extracellular cell wall fragments. A compound with a mass-to-charge ratio in positive ion mode of $(M + H)^+$ 497.204 m/z, corresponding to MurNAc-GlcNAc

(theoretical $(M + H)^+$ 497.1977 m/z; Table S1), which was expected to accumulate in the supernatants of $\Delta namZ$ mutants, was found in only very tiny amounts, albeit about twofold more in the $\Delta namZ$ than in the WT strain (Fig. 1). Rather, another compound accumulated in considerable amounts and about twofold more compared with WT (Fig. 1), which revealed a mass-to-charge ratio $(M + H)^+$ of 754.284 m/z (theoretical $(M + H)^+$ 754.2877 m/z; Table S1), consistent with theoretical exact mass of the trisaccharide MurNAc-GlcNAc-1,6-anhydroMurNAc (MurNAc-GlcNAc-anhMurNAc). This product of peptidoglycan cleavage by a lytic transglycosylase is expected to accumulate in a strain defective for an exo-lytic *N*-acetylmuramidase. This trisaccharide was absent in the $\Delta nagZ$ mutant, which instead accumulated large amounts of GlcNAc-anhMurNAc and to a lesser extent also GlcNAc-MurNAc. Both compounds were unequivocally identified by their $(M + H)^+$ of 479.185 m/z and 497.196 m/z, respectively (Fig. 1) and by *in vitro* cleavage with the recombinant NagZ enzyme (data not shown). GlcNAc-anhMurNAc and GlcNAc-MurNAc disaccharides did not accumulate in the $\Delta namZ$ mutant and the WT strain, which indicates that NagZ is responsible for cleaving GlcNAc-anhMurNAc/

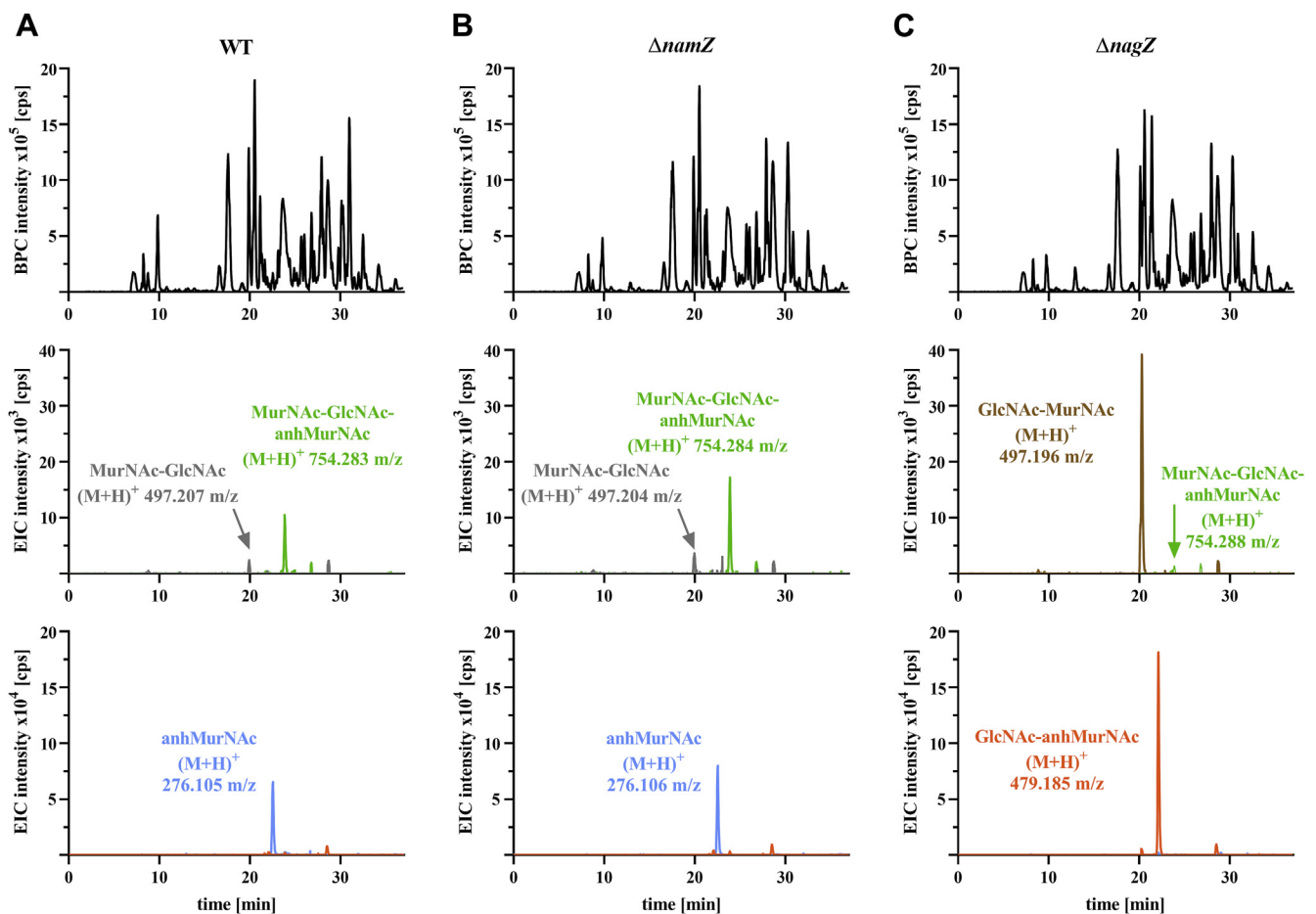


Figure 1. Accumulation of specific cell wall fragments in growth supernatants of *B. subtilis* WT, $\Delta namZ$, and $\Delta nagZ$ cells. Supernatants of stationary phase cultures (grown for 20 h in LB) of *B. subtilis* WT (A), $\Delta namZ$, (B) and $\Delta nagZ$ (C) were analyzed by LC-MS for the accumulation of small cell wall fragments. Shown are the base peak chromatograms (BPCs; black) and extracted ion chromatograms (EIC) for the disaccharides MurNAc-GlcNAc (gray), GlcNAc-MurNAc (brown), GlcNAc-anhMurNAc (orange) as well as anhydroMurNAc (light blue) and the trisaccharide MurNAc-GlcNAc-anhMurNAc (green). To unequivocally identify the accumulation products, these were treated with recombinant NagZ (8).

Exo-muramidase NamZ of *B. subtilis*

GlcNAc-MurNAc. Consistently, an accumulation of anhydromuramic acid ((M + H)⁺ of 276.106 m/z) was observed in the supernatant of WT and $\Delta namZ$ strains but was absent in $\Delta nagZ$. Although the amount of potential NamZ substrates that accumulated in the supernatant of a *B. subtilis* $\Delta namZ$ mutant was surprisingly low, the identity of the small soluble peptidoglycan fragments with a MurNAc entity at the non-reducing end supports our hypothesis that *namZ* encodes a secreted exo-*N*-acetylmuramidase.

Recombinant NamZ forms a dimer in solution

To further characterize NamZ, the enzyme was cloned and heterologously expressed in *E. coli* as C-terminal His₆-tag fusion protein and subsequently purified to apparent homogeneity via Ni²⁺ affinity chromatography followed by size-exclusion chromatography, as revealed by sodium dodecyl sulfate–polyacrylamide gel electrophoresis (SDS-PAGE) analysis (Fig. S2). SDS-PAGE analysis of NamZ under denaturing conditions revealed the monomeric protein, in agreement with the calculated mass of 44.77 kDa. Del Rio and colleagues reported that the exo-*N*-acetylmuramidase entity is an enzyme with an apparent molecular mass of 90 kDa (20), suggesting that the enzyme forms a dimer in solution (Fig. S2). Therefore, we determined the oligomeric state of NamZ in solution. The purified recombinant NamZ protein was subject to size-exclusion chromatography coupled with multiangle light scattering (SEC-MALS). At the peak maximum, NamZ eluted clearly with an apparent mass according to MALS analysis of 89.3 ± 7.4 kDa in three independent experiments (Fig. S2), confirming the expected theoretical mass of 89.54 kDa of the NamZ dimer. Based on SEC-MALS analysis, we concluded that the NamZ protein indeed appears mainly dimeric in solution, consistent with the previous observation (20).

Identification of NamZ as a specific exo-*N*-acetylmuramidase using synthetic substrate pNP-MurNAc

Chromogenic and fluorogenic substrates greatly facilitate the characterization of glycosidases, as they allow the determination of enzymatic activity and specificity with high sensitivity; e.g., the β -galactosidase LacZ of *E. coli* is routinely assayed using ortho-nitrophenyl β -galactopyranoside (oNP-Gal) in the so-called β -Gal assay (28). Similarly, the activity of NagZ of *B. subtilis* had been assayed using chromogenic para-nitrophenyl β -*N*-acetylglucosaminide (pNP-GlcNAc) or, alternatively, the fluorogenic 4-methylumbelliferyl β -*N*-acetylglucosaminide (4MU-GlcNAc) (8, 29, 30). Del Rio *et al.* reported the synthesis and use of the fluorogenic substrate 4MU-MurNAc for the detection of exo- β -*N*-acetylmuramidase activity in the supernatant of *B. subtilis* cultures (20, 31). We decided to synthesize the analogous chromogenic substrate para-nitrophenyl β -*N*-acetylmuramic acid (pNP-MurNAc; para-nitrophenyl 2-acetamido-3-O-(*D*-L-carboxyethyl)-2-deoxy- β -*D*-glucopyranoside), starting from commercially available pNP-GlcNAc in analogy to a previously published procedure (32). In brief, pNP-GlcNAc was transformed into its 4,6-benzylidene derivative followed by alkylation of the 3-OH group using rac-2-chloropropionic acid.

Direct methylation of the carboxyl group allowed purification and separation of the desired diastereomer from the minor *iso*-MurNAc diastereomer. Final deprotection under acidic conditions for the removal of the benzylidene group and basic conditions for methyl ester cleavage resulted in 67% yield of pNP-MurNAc. A similar procedure was followed to isolate para-nitrophenyl 2-acetamido-3-O-(L-1-carboxyethyl)-2-deoxy- β -*D*-glucopyranoside derivative (see supporting information for details). Exo- β -*N*-acetylmuramidase activity of recombinant NamZ was demonstrated by the release of nitrophenolate from the chromogenic substrate pNP-MurNAc (Fig. 2). To determine the specificity of NamZ, the chromogenic substrates pNP-GlcNAc and oNP-GalNAc were also tested. NamZ specifically hydrolyzed pNP-MurNAc, but not the other tested chromogenic substrates, which in turn were specifically cleaved by LacZ and NagZ. This assay identified NamZ as a highly specific exo- β -*N*-acetylmuramidase (Fig. 2).

Biochemical characterization of NamZ using pNP-MurNAc

Prior to the biochemical characterization of NamZ using pNP-MurNAc, we checked the purity of the synthetic substrate with HPLC-MS and NMR. The ¹H- and ¹³C-NMR spectra of the synthetic pNP-MurNAc and pNP-isoMurNAc products indicate that both compounds are of high purity (>95%) (for a detailed description of the synthesis, see supporting information). In the methanolic stock solution of pNP-MurNAc used for enzyme reactions, the main compounds in the base peak chromatogram (BPC) observed by MS analysis showed a mass of (M + H)⁺ 415.132 m/z (retention time of 36.7 min) corresponding to the theoretical mass of pNP-MurNAc ((M + H)⁺ 415.1347 m/z; cf. Table S1). Occasionally we found an additional small peak at a retention time of 40.3 min with a mass of (M + H)⁺ 429.147 m/z, identified as methylated pNP-MurNAc (theoretical mass (M + H)⁺ 429.1504 m/z; cf. Table S1), which may have resulted from esterification of the acidic pNP-MurNAc in the prepared stock solution in MeOH. Since traces of the methylated pNP-MurNAc may inhibit the NamZ reaction, the methylation was removed by preincubation of the pNP-MurNAc substrate for 30 min at pH 8.0 prior to the NamZ reactions.

We determined stability and reaction optima of recombinant NamZ at temperatures between 4 and 60 °C and pH values between 2 and 10, using the chromogenic substrate pNP-MurNAc. Stability was measured by the loss of activity of NamZ after 30 min of preincubation at different temperatures or pH conditions, and the optima were determined by direct reactions of NamZ at different temperature or pH conditions. NamZ was shown to be stable from 4 °C to 37 °C, with a short-term maximal activity at around 37 °C (Fig. S3). NamZ was also shown to be mostly stable over a pH range from 6.0 to 10.0, with a short-term maximal activity between pH 6.0 and 8.0 (Fig. S3). Furthermore, NamZ retained its activity for several months after purification when stored at either –20 °C or 4 °C. We chose to determine the kinetic parameters of NamZ at 37 °C and in the pH range between 7.0 and 8.0, which represents the optimal pH condition in respect to

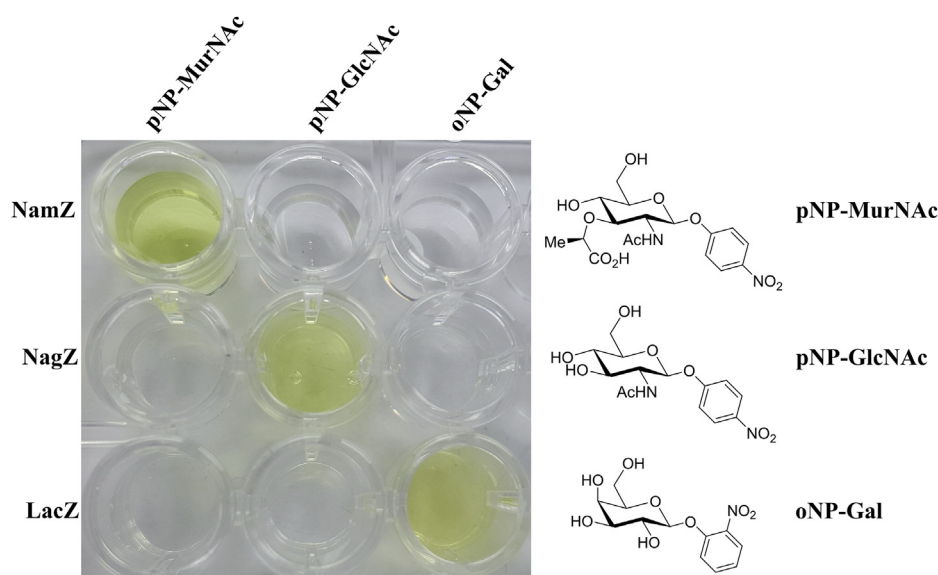


Figure 2. NamZ of *B. subtilis* specifically cleaves the chromogenic substrate pNP-MurNAc. The other tested chromogenic substrates, pNP-GlcNAc and oNP-Gal were not cleaved by NamZ, but are substrates of the exo- β -*N*-acetylglucosaminidase of *B. subtilis* (NagZ) and the β -*D*-galactosidase of *E. coli* (LacZ), respectively. Purified recombinant NamZ and NagZ from *B. subtilis*, as well as commercial LacZ (100 μ g/ml each) were incubated for 30 min with the indicated chromogenic compound (100 μ M each). Color intensity was enhanced by adding an equal volume of sodium borate buffer (100 mM, pH 10).

stability and activity. Kinetic parameters for the chromogenic substrate were calculated using a standard curve for para-nitrophenol (Fig. 3A). The maximal velocity of the reaction of NamZ with the chromogenic substrate pNP-MurNAc was determined as k_{cat} of 1.08 s^{-1} (v_{max} of $1.45 \mu\text{mol min}^{-1} \text{ mg}^{-1}$) and the Michaelis–Menten constant as K_{M} of 0.125 mM at 37 °C.

Preparation of MurNAc-GlcNAc from peptidoglycan enzymatic digests

We aimed to biochemically characterize NamZ further, using the disaccharide MurNAc-GlcNAc, the proposed minimal natural substrate. To prepare MurNAc-GlcNAc, peptidoglycan isolated from *B. subtilis* was digested with recombinant muramyl-L-alanine amidase (CwlC of *B. subtilis*) and endo-*N*-acetylglucosaminidase (Atl^{Glc} of *S. aureus*) as described elsewhere (15, 33). The crude enzyme digest contained large amounts of the disaccharide MurNAc-GlcNAc, as revealed by LC-MS analysis, but also cross-linked, non-cross-linked peptides and other saccharides in minor amounts. Therefore, the disaccharide was purified using semipreparative HPLC, yielding a MurNAc-GlcNAc preparation that was mostly free of tri- and tetrapeptides as well as cross-linked tri-tetrapeptides as shown by LC-MS analysis (Fig. S4). The mass spectrum of the MurNAc-GlcNAc pool, appearing at retention time of 21.2 min, contained solely the molecule mass $(M + H)^+$ 497.196 m/z, confirming that the MurNAc-GlcNAc preparation was of sufficient purity (Fig. S4C).

Biochemical characterization of NamZ using MurNAc-GlcNAc

Using the purified natural minimal substrate MurNAc-GlcNAc, NamZ activity was characterized. The disaccharide

$(M + H)^+$ 497.196 m/z, retention time of 21.1 min) completely disappeared by adding recombinant NamZ (Fig. S5A) and two new peaks appeared, which were identified as MurNAc (measured mass $(M + H)^+$ 294.118 m/z, retention time of 21.8 min) and GlcNAc (measured mass $(M + H)^+$ 222.097 m/z, retention time of 10.0 min) (Fig. S5B).

NamZ requires a MurNAc entity at the nonreducing end, since GlcNAc-MurNAc was not cleaved as shown by LC-MS (determined $(M + H)^+$ 497.198 m/z, retention time of 21.8 min) (Fig. S6). In contrast, NagZ readily cleaved GlcNAc-MurNAc but not MurNAc-GlcNAc. After incubation with NagZ, the GlcNAc-MurNAc peak completely disappeared and two new peaks appeared that correspond to GlcNAc (measured mass $(M + H)^+$ 222.097 m/z, retention time of 10.0 min) and MurNAc (measured mass $(M + H)^+$ 294.118 m/z, retention time of 21.8 min) (Fig. S6).

To determine the kinetic parameters of NamZ with MurNAc-GlcNAc as a substrate, we chose a pH of 7.0 for the assay. For MurNAc-GlcNAc, the release of MurNAc by the action of NamZ was analyzed using HPLC-MS. Therefore, a standard curve for MurNAc (Fig. 3B) was created and kinetic parameters for the natural minimal substrate were calculated (Fig. 3C). The reaction of NamZ with MurNAc-GlcNAc as a substrate at pH 7.0 was much faster than with the chromogenic substrate pNP-MurNAc at pH 8.0 (k_{cat} of 66.25 and 1.08 s^{-1} ; v_{max} of 88.64 and $1.45 \mu\text{mol min}^{-1} \text{ mg}^{-1}$) but the K_{M} for MurNAc-GlcNAc was a 30-fold higher than that for pNP-MurNAc (3.59 and 0.125 mM). With MurNAc-GlcNAc as a substrate, a first saturation was reached at a substrate concentration of 0.2 mM substrate. After this saturation, the curve increased again until the second saturation at a substrate concentration of 6 mM was reached. Because of these two saturations, the kinetic parameters for 0.2 mM MurNAc-

Exo-muramidase NamZ of *B. subtilis*

GlcNAc as the highest concentration were also calculated. Hence, a k_{cat} of 4.48 s^{-1} (v_{max} of $5.99 \mu\text{mol min}^{-1} \text{mg}^{-1}$) and a K_{M} of 0.22 mM were determined (Fig. 3D).

Sequential digest of peptidoglycan by NagZ, AmiE, and NamZ

We further tested whether the exo- β -*N*-acetylglucosaminidase NagZ, the *N*-acetylmuramyl-L-alanine amidase AmiE, and NamZ together could digest intact *B. subtilis* 168 peptidoglycan. To this end, purified peptidoglycan was incubated with all three purified recombinant enzymes overnight and the generated products were analyzed using HPLC-MS in negative and positive ion mode. Analysis of degraded peptidoglycan revealed single cell wall carbohydrates and peptides (Fig. 4). We could identify the monosaccharides GlcNAc (observed mass of $(\text{M} + \text{H})^+$ 222.098 *m/z*, retention time of 10.1 min), MurNAc $(\text{M} - \text{H})^-$ 292.104 *m/z*, 21.7 min) and anMurNAc $(\text{M} - \text{H})^-$ 274.094 *m/z*, 24.8 min). Furthermore, peptides were identified as tripeptide with an amidation $(\text{M} - \text{H})^-$ 388.187 *m/z*, 8.5 min), cross-linked tri-tetrapeptide with two amidations $(\text{M} - \text{H})^-$ 830.406 *m/z*, 12.1 min), and cross-linked tri-tetrapeptide with one amidation $(\text{M} - \text{H})^-$ 831.388 *m/z*, 15.1 min)

(Fig. 4). Additionally, the mass spectra of the carbohydrates and peptide peaks were analyzed to confirm the identities of the hydrolysis products (Fig. S7). When peptidoglycan was digested with one of the three enzymes alone, only low amounts of cell wall monosaccharides and peptides could be identified. Hence, the joint and coordinated activity of all three enzymes NagZ, AmiE, and NamZ, is needed to digest the peptidoglycan, thereby releasing the respective peptidoglycan-derived monosaccharides and peptides.

Structure model of NamZ reveals unique glycosidase fold

NamZ shares significant homology with two proteins from *Bacteroides fragilis* NCTC 9343, BF0379 (40% sequence identity, PDB ID 4jja) and BF0371 (44% sequential identity, PDB ID 4k05), the structures of which were determined and deposited in the Protein Data Bank (Joint Center for Structural Genomics). Hitherto, nothing is known about the biological function of these proteins. We built a homology model of NamZ based on these structures, using HHPred (34) (Fig. 5). Even though NamZ shares higher overall sequence homology with BF0371, the residues around the putative active site of

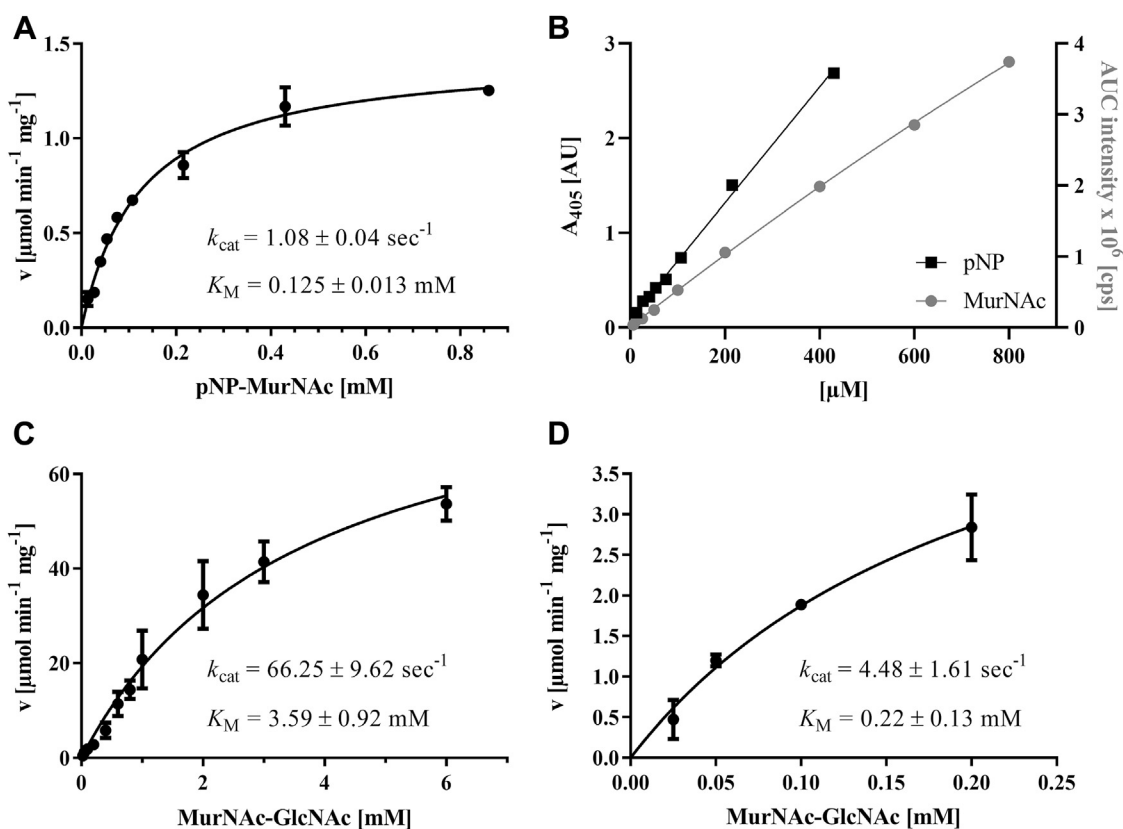


Figure 3. Determination of the kinetic parameters of NamZ using the chromogenic substrate pNP-MurNAc at pH 8.0 and MurNAc-GlcNAc substrate at pH 7.0. A, kinetic parameters using the chromogenic substrate pNP-MurNAc were determined as described in Experimental procedures. B, standard curve for 4-nitrophenol (13–430 μM) was determined in 0.2 M phosphate buffer (pH 8.0) (black squares). Absorption of pNP was measured at 405 nm. For all experiments, standard errors (SEM) are indicated and calculated out of three biological replicates. Standard curve for MurNAc (6.25–800 μM) was determined in 0.2 M phosphate buffer (pH 7.0) and stopping buffer (1% formic acid, 0.5% ammonium formate, pH 3.2) in equal amounts in a total volume of 50 μl . Samples were analyzed using HPLC-MS and the areas under the curve (AUCs) were generated using the extracted ion chromatograms (EICs) intensities for MurNAc $(\text{M} - \text{H})^-$ 292.113 *m/z*) (gray circles). C, kinetic parameters using purified MurNAc-GlcNAc were determined. Standard errors (SEM) are indicated and calculated out of three biological replicates. D, kinetic parameters using purified MurNAc-GlcNAc as substrate were determined for substrate concentrations from 0.025 to 0.2 mM as described in Experimental procedures. Standard errors (SEM) are indicated and calculated out of three biological replicates.

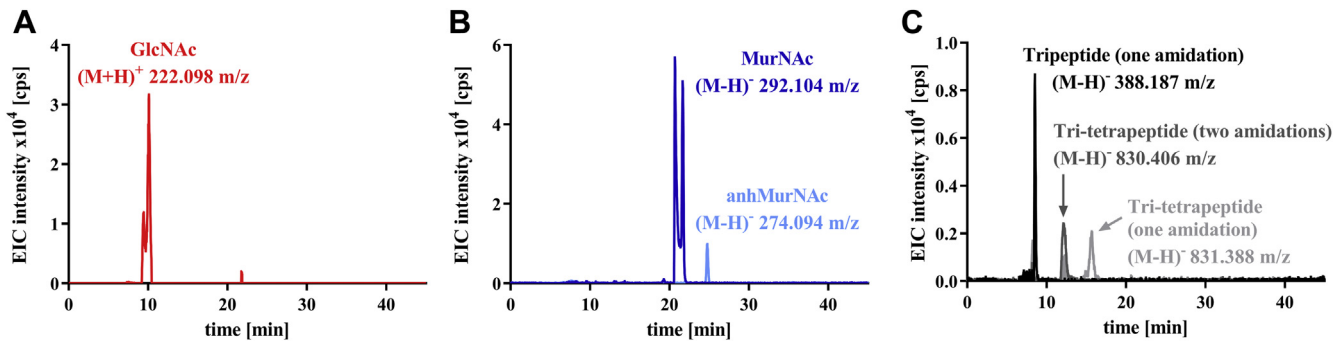


Figure 4. Sequential digest of peptidoglycan by NagZ, NamZ, and AmiE. Purified peptidoglycan was sequentially digested by the action of NagZ, NamZ, and AmiE and analyzed by HPLC-MS. Main products are shown as extracted ion chromatograms (EIC). Single cell wall carbohydrates could be identified with observed masses (A) $(M + H)^+$ 222.098 m/z for GlcNAc (red) with a retention time of 10.1 min, (B) $(M - H)^-$ 292.104 m/z for MurNAc (dark blue) with a retention time of 21.7 min and $(M - H)^-$ 274.094 m/z for anhMurNAc (light blue) with a retention time of 24.8 min. C, peptides could be identified with observed masses $(M - H)^-$ 388.187 m/z for tripeptide with an amidation (black) with a retention time of 8.5 min, $(M - H)^-$ 830.406 m/z for tri-tetrapeptide with two amidations (dark gray) with a retention time of 12.1 min, and $(M - H)^-$ 831.388 m/z for tri-tetrapeptide with one amidation (light gray) with a retention time of 15.1 min.

NamZ and BF0379 are more conserved, suggesting that BF0379 and NamZ may share a very similar function. NamZ consists of two domains, an N-terminal catalytic domain (34–258) and a C-terminal auxiliary domain (259–414). The N-terminal catalytic domain has an $\alpha/\beta/\alpha$ three-layer sandwich architecture with a central parallel β -sheet topology of 321456 (order of β -strands in the sheet). A putative catalytic residue (Glu92) is located at the C-terminal end of the second β -strand. The C-terminal auxiliary domain has an α/β architecture with three strands. A putative active site cavity is formed between the domain interface defined by both domains. A positive charged arginine (Arg279) from this C-terminal domain points toward the cavity. Surprisingly, the catalytic domain has a Rossmann-like fold, which is usually involved in binding nucleotides. However, the proposed catalytic domain of NamZ does not process the glycine-rich signature of a nucleotide-binding motif. Moreover, the Rossmann-like region is partially occupied by its C-terminal region of the catalytic domain (residues 245–251).

Distribution of NamZ and other recycling enzymes

A phylogenetic tree displaying the distribution of recycling associated enzymes, including NamZ, was built as described in [Experimental procedures](#). Proteins with significant sequence identities to the selected recycling proteins can be found in a wide range of bacterial taxa (Fig. 6). Interestingly, NamZ occurs mainly in the phylum of *Bacteroidetes* (in e.g., *Tannerella forsythia*, *B. fragilis* and *Porphyromonas gingivalis*) and less frequently within Spirochetes (e.g., *Treponema denticola*, *Leptospira interrogans*), *Bacilli* (*B. subtilis*), *Clostridia* (*Clostridium acetobutylicum*), *Actinobacteria* (*Amycolatopsis mediterranei*, *Brachybacterium faecium*), and γ -proteobacteria (*Yersinia enterocolitica*). Furthermore, the occurrence of NamZ is mostly coupled to the presence of NagZ, whereas NagZ appears also without NamZ. Also, NamZ and the MurNAc-6P etherase MurQ can be usually found together in the bacterial genomes, since NamZ generates a “precursor substrate” for MurQ. We recently reported on a family of exo-lytic 6-phospho-muramidase that includes MupG of *S. aureus* (www.cazy.org/GH17_0.html), which specifically hydrolyzes β -1,4-MurNAc-6P

entities from the nonreducing end of the disaccharide MurNAc6P-GlcNAc (15). Analysis of the phylogenetic distribution of MupG-like proteins revealed that whenever a putative MurNAc-6P hydrolase is present, NamZ is missing (Fig. 6). Considering the complementary functions of the both enzyme families, NamZ and MupG, this observation is reasonable. A characteristic recycling route, the anabolic recycling involving the MurNAc-6P phosphatase MupP, the anomeric MurNAc

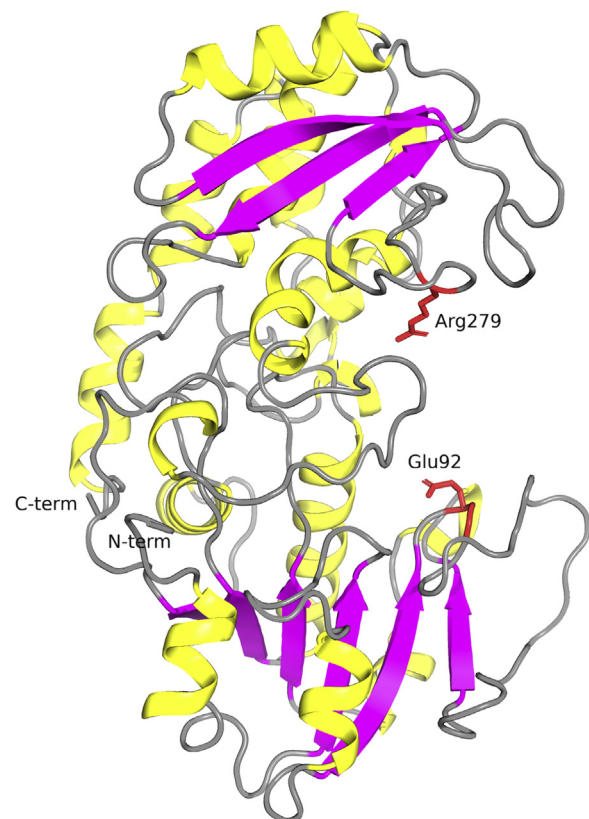


Figure 5. A structure model of *B. subtilis* NamZ depicts a novel glycosidase-fold. A structural model of NamZ, constructed by HHPred, reveals a putative active site located in a cleft within the interface of two sub-domains. The N-terminal catalytic domain contains a Rossmann-fold-like domain (lower part) and contains a conserved glutamate (Glu92) at the tip of the second β -strand. The C-terminal auxiliary domain contains a highly exposed conserved arginine (Arg279).

Exo-muramidase NamZ of *B. subtilis*

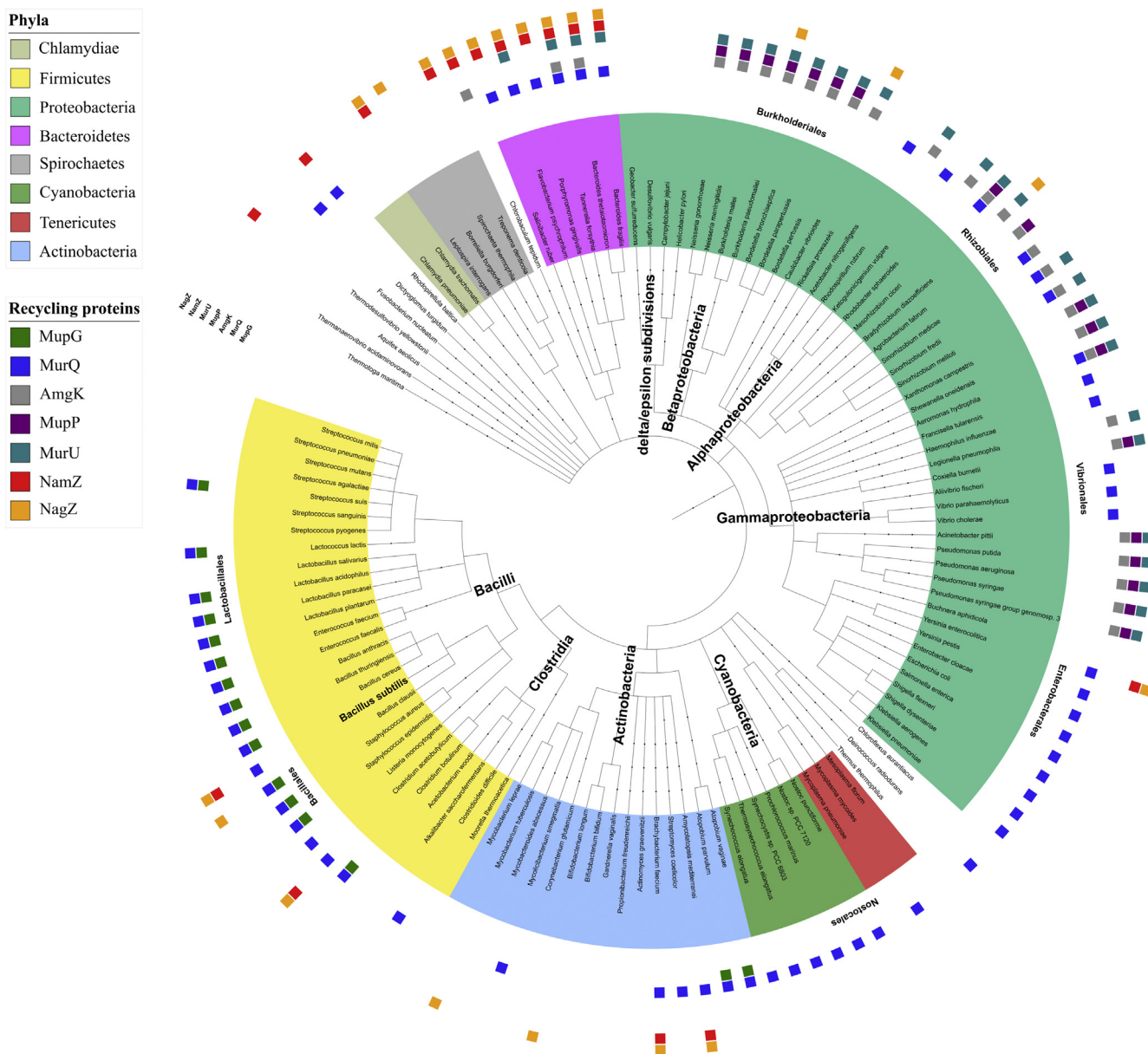


Figure 6. Phylogenetic tree showing the distribution of peptidoglycan recycling associated proteins in representative bacterial taxa. MurQ (blue) is a representative enzyme of the MurQ pathway present in *E. coli* and *B. subtilis* (16, 21, 22), and MupG (green) is a representative of the modified MurQ pathway identified in *S. aureus* (15). AmgK (gray), MupP (purple), and MurU (teal) are representatives of an alternative, “anabolic” recycling pathway described in *P. putida* (35). NagZ (orange) and NamZ (red) pinpoint the putative presence of autolytic pathways described in *B. subtilis* (16). The tree is built on the taxonomy according to NCBI and MultiGeneBlast searches for these proteins, using the studies by (35, 50) as reference.

kinase AmgK, and the MurNAc- α -1P uridylyltransferase MurU has been recently identified in *Pseudomonas* sp. and a range of other Gram-negative bacteria, including *Bacteroides* sp. (35). Analysis of the phylogenetic distribution of recycling enzymes revealed that whenever the anabolic peptidoglycan recycling route is present, NamZ is mostly missing. Thus, NamZ constitutes a peptidoglycan degradative enzyme characteristic for a subset of bacterial species, which process peptidoglycan by a distinct route that is different from other species lacking NamZ.

Discussion

In this study, *ybbC* (*namZ*) of *B. subtilis* was identified as the first known gene encoding an exo-*N*-acetylmuramidase that

specifically cleaves non-reducing terminal MurNAc from synthetic and peptidoglycan-derived natural glycosides. Several lines of evidence indicate that NamZ is identical to the exo- β -*N*-acetylmuramidase that had been partially purified from the supernatant of stationary phase cultures of *B. subtilis* and characterized by Del Rio and colleagues in the 1970s (19, 20, 31). First, the authors reported that the exo- β -*N*-acetylmuramidase is coexpressed with an exo- β -*N*-acetylglucosaminidase, which was later identified as NagZ (16, 20). This is consistent with the location of *ybbC* (*namZ*) in an operon next to the exo- β -*N*-acetylglucosaminidase *nagZ* (*ybbD*) and joint regulation of both genes *via* the transcriptional regulator MurR (YbbH) and catabolite repression (16, 21, 25). Analysis of growth of Δ *namZ* and Δ *nagZ* mutants and the

accumulation of specific turnover fragments, occurring in stationary phase as shown in this study, further supports that NamZ is coexpressed with NagZ. Second, exo-muramidase activity was identified in the growth medium of *B. subtilis* WT but not of $\Delta namZ$ mutant cells, consistent with the putative signal peptide sequence identified in the amino-terminus of the NamZ preprotein and with the previously reported localization and association with cell wall material (20). Third, we showed that NamZ mainly associates in solution to form dimers of two 44.77 kDa monomers, consistent with the reported molecular weight of 90 kDa described for the exo- β -*N*-acetylmuramidase by Del Rio *et al.* (20). Fourth, biochemical characteristics and kinetic parameters determined for NamZ further affirm its identity with the exo- β -*N*-acetylmuramidase entity reported by Del Rio *et al.* (19, 20). Del Rio showed the partially purified exo- β -*N*-acetylmuramidase to be maximal active and stable at a pH of 8.0, similarly to our results, which showed an optimum activity of NamZ between pH 6.0 and 8.0 and an optimum stability within the range of pH 6.0–10.0. Furthermore, although we used a slightly different artificial substrate with an altered aglycon, the biochemical and kinetic parameters we determined for recombinant NamZ with pNP-MurNAc (K_M 125 μ M; v_{max} 1.45 μ mol min⁻¹ mg⁻¹) were very similar to those defined by Del Rio *et al.* using 4MU-MurNAc as substrate (K_M 190 μ M; v_{max} 1.5 μ mol min⁻¹ mg⁻¹) (20). The kinetic parameters we determined for MurNAc-GlcNAc, however, differed from those reported by Del Rio *et al.* (20), when the full substrate concentrations range from 0.025 to 6 mM was considered (K_M 3.6 mM; v_{max} 88.64 μ mol min⁻¹ mg⁻¹). Thus, the enzyme appears to have lower affinity to the substrate MurNAc-GlcNAc (high K_M), but is more active than previously reported (K_M 650 μ M and v_{max} 16.29 μ mol min⁻¹ mg⁻¹) (20). However, we observed a biphasic kinetic behavior with this substrate and if calculating the parameters only for the first saturation, including concentrations up to 0.2 mM MurNAc-GlcNAc (Fig. 3D), we obtained kinetic parameters (K_M 220 μ M; v_{max} 5.99 μ mol min⁻¹ mg⁻¹) more similar to those reported previously (20). The reason for this discrepancy is not clear but may result from compounds that may have been copurified with the MurNAc-GlcNAc in our or Del Rio's preparation that affect NamZ activity. We used a similar protocol for substrate preparation, involving peptidoglycan cleavage by the *N*-acetylglucosaminidase AtI^{Glc} of *S. aureus* as well as the subsequent purification of the MurNAc-GlcNAc by liquid chromatography. However, the source of peptidoglycan differed in both preparations, ours was from *B. subtilis*, whereas Del Rio *et al.* used peptidoglycan from *Micrococcus luteus* (20). The major difference is that we removed the peptide stems from the peptidoglycan preparation by treatment with the amidase CwlC from *B. subtilis*, whereas Del Rio only relied on the endogenous amidase present in the *M. luteus* preparation. Although our MurNAc-GlcNAc preparation appears reasonably pure, we cannot exclude that we copurified some cell-wall-derived compounds that may affect NamZ kinetics.

The disaccharide MurNAc- β -1,4-GlcNAc likely represents the minimal natural substrate of NamZ. Surprisingly, however,

only very little amounts of MurNAc-GlcNAc accumulated in the culture medium of the $\Delta namZ$ mutant. The reason for this unexpected result is unclear but we are currently investigating whether MurNAc-GlcNAc can be taken up and metabolized by *B. subtilis*. Instead, in the growth medium of the $\Delta namZ$ mutant, significant amounts of MurNAc-GlcNAc-anhMurNAc trisaccharide accumulated, about twice the amount that accumulated in the WT strain. Although, the accumulation of the trisaccharide in the WT may indicate that NamZ does not efficiently cleave the anhMurNAc-containing trisaccharide, the MurNAc-GlcNAc-anhMurNAc accumulation product was completely cleaved *in vivo* if recombinant NamZ was added yielding MurNAc and GlcNAc-anhMurNAc products. Thus, cleavage of the non-reducing terminal MurNAc of the trisaccharide by NamZ is, at least in part, responsible for the generation of GlcNAc-anhMurNAc, which accumulated in a huge amount in a $\Delta nagZ$ mutant. Besides approximately tenfold lower levels of GlcNAc-MurNAc occur in this mutant. This indicates that, firstly, NagZ is crucial for the extracellular cleavage of GlcNAc-anhMurNAc and GlcNAc-MurNAc in *B. subtilis*, and, secondly, no uptake of these disaccharides occurs through the cell membrane. The absence of GlcNAc-anhMurNAc and GlcNAc-MurNAc in the culture supernatants of the $\Delta namZ$ mutant indicates that NamZ is responsible, directly or indirectly, for the generation of these NagZ substrates. Since the amount of MurNAc-GlcNAc-anhMurNAc is rather low, this trisaccharide may not be the main source of GlcNAc-anhMurNAc.

It may be assumed that primarily long-chain peptidoglycan fragments accumulate in the supernatant of a $\Delta namZ$ mutant, which are not easily accessible by LC-MS due to their large sizes. Indeed, NamZ as well as NagZ occurs associated with cell wall material and possibly acts in concert to degrade peptidoglycan. Our results showed that the exo-lytic *N*-acetylglucosaminidase NagZ and the exo-muramoyl-L-alanine amidase AmiE, along with NamZ, can digest intact peptidoglycan, by sequential hydrolysis. However, the rather low amount of thereby released fragments suggests that the decay is not quantitative and likely blocked by structural constraints within the peptidoglycan, such as de-*N*-acetylation. We suppose that the peptidoglycan in *B. subtilis* is autolytically cleaved during vegetative growth by a concerted action of endo-acting as well as disaccharide producing glycosidases (lytic transglycosylases, endo- β -*N*-acetylmuramidases, and β -*N*-acetylglucosaminidases), which yield GlcNAc-anhMurNAc, GlcNAc-MurNAc, and MurNAc(-peptide)-GlcNAc as the final turnover products (Fig. 7). Consistently, we observed an accumulation of GlcNAc-anhMurNAc and GlcNAc-MurNAc in the supernatants of a $\Delta nagZ$ mutant, and an accumulation of MurNAc-GlcNAc in a $\Delta namZ$ mutant, which however, as mentioned above, is not found in the culture supernatant since the disaccharide may be readily transported into the cells. Candidate peptidoglycan-lytic enzymes, which generate these putative substrates of AmiE, NamZ, and NagZ, may be the bifunctional lytic transglycosidase/muramidase CwlQ (YjbJ) and the exo-acting *N*-acetylglucosaminidase LytG of *B. subtilis* (36, 37). Altogether, these enzymes yield the monosaccharides

Exo-muramidase NamZ of *B. subtilis*

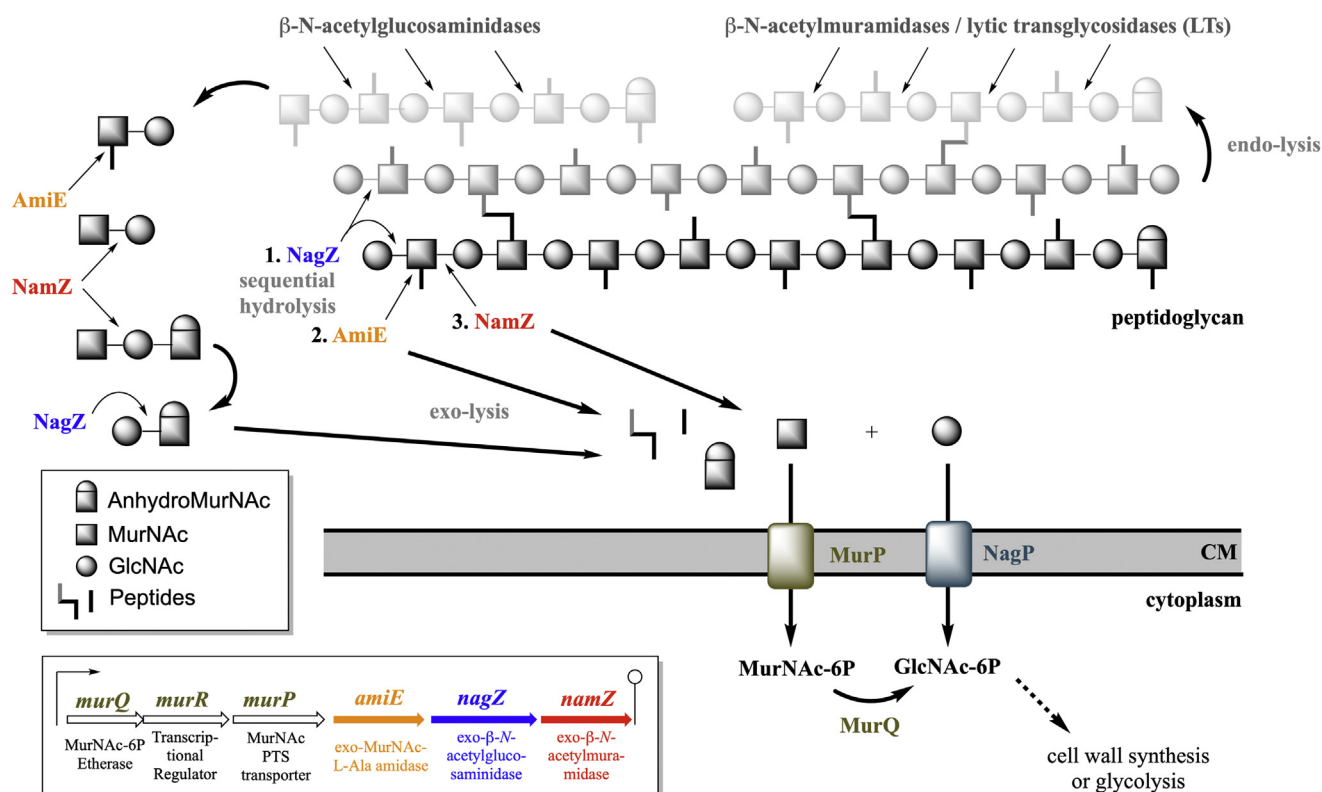


Figure 7. Overview of the roles of NagZ, AmiE, and NamZ of the peptidoglycan recycling/MurNAc catabolic operon in the degradation of peptidoglycan in *B. subtilis*. The exo-lytic peptidoglycan hydrolases NagZ (exo- β -*N*-acetylglucosaminidase), AmiE (exo-*N*-acetylmuramyl-L-alanine amidase), and NamZ (formerly YbbC; exo- β -*N*-acetylmuramidase) cleave-off GlcNAc, peptides, and MurNAc residues, respectively, from the nonreducing terminus of peptidoglycan chains by sequential reactions, as indicated (1. NagZ, 2. AmiE, and 3. NamZ). Furthermore, these enzymes may act on shorter fragments released from the peptidoglycan by the action of endo-lytic and disaccharide-releasing exo-lytic autolysins. Apparently, NamZ primarily cleaves MurNAc-GlcNAc and MurNAc-GlcNAc-anhMurNAc, whereas NagZ cleaves GlcNAc-anhMurNAc and GlcNAc-MurNAc. Thereby released monosaccharides, MurNAc and GlcNAc, are recovered by *B. subtilis* via the phosphotransferase system transporters MurP and NagP, yielding in the cytoplasm MurNAc 6-phosphate (MurNAc-6P) and GlcNAc 6-phosphate (GlcNAc-6P), respectively. The MurNAc-6P lactyl ether hydrolase (etherase) MurQ converts MurNAc-6P to GlcNAc-6P in the cytoplasm, which enters pathways leading to either cell wall synthesis or glycolysis.

GlcNAc and MurNAc, which are taken up and phosphorylated by the PTS transporters MurP and NagP, respectively, and further catabolized intracellularly, in a process known as peptidoglycan turnover and recycling (16, 21). Intracellular MurNAc-6P is converted to GlcNAc-6P by MurQ further entering glycolysis or the cell wall *de novo* synthesis pathway (Fig. 7). Consistent with the expression of AmiE, NamZ, and NagZ, the accumulation of MurNAc-6P occurs during late exponential, transition, and stationary phase as reported previously (21).

The exo-*N*-acetylmuramidase NamZ previously belonged to a protein family of so far unknown function (DUF1343) that showed no significant amino acids sequence identity with other glycosidases. A homology model of NamZ that was constructed based on crystal structures of two DUF1343 proteins, BF0379 and BF0371 from *B. fragilis* NCTC 9343, revealed an atypical glycosidase-fold (Fig. 5). A putative active site cleft is located within the interface constituted by two subdomains, an N-terminal Rossmann-fold-like domain and a C-terminal auxiliary α/β domain. Even though NamZ shares higher overall sequence homology with BF0371, the residues around the putative active site of NamZ and BF0379 are more conserved, suggesting that BF0379 and NamZ may share a very similar function. Although the Rossmann-fold-like domain is atypical for glycosidases, the

distinguished families 4 and 109 of glycosidases also contain a Rossmann-like-domain fold (<https://www.cazy.org>). These glycosidases operate by an unusual mechanism that involves an NAD^+ cofactor required for cleavage of the glycosidic bond *via* an oxidation/reduction step (38–41). This unique glycosidase mechanism is, however, incompatible with exo-*N*-acetylmuramidase function, since MurNAc contains a lactyl ether substituent at C3 and not a hydroxyl group. Moreover, we obtained no evidence whatsoever that NamZ function depends on NAD^+ and divalent cations, suggesting that the Rossmann-like-fold in DUF1343 enzymes does not involve an NAD^+ cofactor and a redox-step. Thus, NamZ represents a novel example of a classic fold evolved to adopt new glycoside hydrolase activity. Although some members of glycoside hydrolases (*e.g.*, GH4 and GH109) make use of NAD^+ as a cofactor that binds to a Rossmann-fold domain, to the best of our knowledge, there is no known example of glycoside hydrolase activity arising from a Rossmann-like fold itself. Interestingly, many Rossmann-fold enzymes utilizing nucleoside-based cofactors contain a carboxylate side chain at the tip of the second β -strand (β 2-Asp/Glu) for ribose-binding interaction (42), which apparently is conserved in NamZ. Thus, NamZ may represent a novel example of a classic fold evolved to adopt new glycoside hydrolase activity. Further studies exploring the structure/

mechanism of the NamZ family of glycosidases are needed to clarify this issue.

NamZ is a member of a large protein family (pfam PF07075) with presently 2300 predominately bacterial members that have no known function. Thus, NamZ defines a novel family of glycoside hydrolases that have a distinctive structure and possibly mechanism compared with previously known GHs cataloged by the CAZy database (newly classified as GH171; www.cazy.org/GH171.html). Intriguing, *B. subtilis* is an exception since only very few Firmicutes or Gram-positive bacteria, in general, possess a NamZ protein, which is mostly found in the Bacteroidetes phylum (Fig. 6). Importantly, this study fills the gap of the *namZ* (*ybbC*) gene in the peptidoglycan recycling and MurNac catabolic operon and provides insights into the role of NagZ, AmiE, and NamZ in peptidoglycan turnover by characterizing its NamZ glycosidase protein product and assigning its unique exo-muramidase function.

Experimental procedures

Chemicals, media, enzymes, and oligonucleotides

Chemicals were obtained from AppliChem GmbH, Bachem, Carbosynth Ltd, Serva Electrophoresis GmbH, Sigma-Aldrich, Thermo Fisher Scientific, Carl Roth GmbH + Co. KG, and VWR. Antibiotics were received from Sigma-Aldrich and lysogeny broth medium (LB broth Lennox) was from Carl Roth GmbH + Co. KG. DNA polymerases and enzymes for DNA restriction and cloning were from Genaxxon bioscience GmbH, New England Biolabs, and Thermo Fisher Scientific. The Gene JET Genomic DNA Purification Kit, Plasmid Miniprep Kit, PCR Purification Kit, and GeneRuler 1-kb marker were also from Thermo Fisher Scientific. Oligonucleotides and sequencing results were received from MWG Eurofins.

Bacterial strains and growth conditions

The bacterial strains and plasmids used in this study are listed in Table 1. For the generation of markerless *B. subtilis*

168 Δ nagZ and Δ namZ mutants, the loop-out plasmid pDR244 was used to excise the erythromycin resistance cassettes flanked by *loxP* sites in strains *B. subtilis* 168- Δ nagZ::erm and *B. subtilis* 168- Δ namZ::erm, received from the *Bacillus* Genetic Stock Center, following a published protocol for constructing markerless deletions. In brief, the preparation of naturally competent cells and transformation of pDR244, carrying the *cre* recombinase gene, was accomplished using MGE medium (43), followed by selection on spectinomycin (100 μ g/ml) and incubation at 30 °C overnight. Transformant colonies were shifted to incubation at 42 °C overnight on LB without added antibiotic. Growing colonies were streaked out on LB, spectinomycin (100 μ g/ml), and erythromycin (5 μ g/ml) to verify *cre*-dependent loss of the erythromycin resistance cassette and plasmid curing. Colonies growing only on LB were confirmed for the loss of the erythromycin resistance cassette by PCR using *B. subtilis* Δ nagZ and *B. subtilis* Δ namZ chromosomal DNA and primers flanking the regions of interest (nagZ_500_fw and nagZ_500_rev for Δ nagZ as well as namZ_500_fw and namZ_500_rev for Δ namZ; Table S2) as well as DNA sequencing of the amplicons. All strains were cultured under aerobic conditions at 37 °C in LB under continuous shaking at 140 rpm. Antibiotics were used when appropriate at the following concentrations (50 μ g/ml kanamycin or 100 μ g/ml ampicillin).

Analysis of supernatants of *B. subtilis* WT, Δ namZ, and Δ nagZ cells

B. subtilis wild-type, Δ namZ, and Δ nagZ cells were grown for 20 h under constant shaking. Afterward, 1 ml cell cultures were harvested and centrifuged at 12,000g for 10 min at room temperature and 100 μ l of the cell-free supernatant was added to 900 μ l of ice-cold acetone. Samples were mixed by inverting the tubes three times. Following precipitation, the samples were centrifuged at 12,000g for 10 min. The supernatants were dried at 55 °C (SpeedVac, Christ, RVC2-18), and the resulting

Table 1
Strains and plasmids

Strains and plasmids	Genotype and cloning strategy	Reference or source
<i>E. coli</i> DH5 α	<i>supE44 hsdR17 recA1 endA1 gyrA96 thi-1 relA1</i>	New England Biolabs
<i>E. coli</i> BL21 (DE3)	F- <i>ompT hsd SB(rB-mB-) gal dcm</i> (DE3)	New England Biolabs
<i>B. subtilis</i> 168 (WT)	<i>trpC2</i>	<i>Bacillus</i> Genetic Stock Center (BGSCID 1A1)
<i>B. subtilis</i> 168- Δ nagZ::erm	<i>trpC2</i> Δ nagZ::erm	<i>Bacillus</i> Genetic Stock Center (BGSCID BKE01660)
<i>B. subtilis</i> 168- Δ namZ::erm	<i>trpC2</i> Δ namZ::erm	<i>Bacillus</i> Genetic Stock Center (BGSCID BKE01650)
<i>B. subtilis</i> 168- Δ nagZ	<i>trpC2</i> Δ nagZ	this study
<i>B. subtilis</i> 168- Δ namZ	<i>trpC2</i> Δ namZ	this study
<i>S. aureus</i> USA300 JE2	USA300 LAC, cured for three plasmids for antibiotic resistance	(49)
Plasmids		
pDR244	loop-out plasmid, ori _{PACYC} , <i>cre</i> , <i>cop</i> , <i>repF</i> , Amp ^R (<i>E. coli</i>), Spec ^R (<i>B. subtilis</i>)	<i>Bacillus</i> Genetic Stock Center (BGSCID ECE274)
pET29b	<i>E. coli</i> expression vector, Km ^R	Novagen
pET29b- <i>namZ</i>	IPTG-inducible cytoplasmic NamZ-His ₆ expression vector	this study
pET28a	<i>E. coli</i> expression vector, Km ^R	Novagen
pET28a- <i>cwlC</i>	IPTG-inducible cytoplasmic CwlC-His ₆ expression vector	this study
pET28a- <i>atl</i> ^{Glc}	IPTG-inducible cytoplasmic Atl ^{Glc} -His ₆ expression vector	this study
pET22b	<i>E. coli</i> expression vector, Amp ^R	Novagen
pET22b- <i>amiE</i>	IPTG-inducible periplasmic AmiE-His ₆ expression vector	this study
pET16b	<i>E. coli</i> expression vector, Amp ^R	Novagen
pET16b- <i>BsnagZ</i>	IPTG-inducible cytoplasmic BsNagZ-His ₁₀ expression vector	(8, 16)

Amp, ampicillin; Spec, spectinomycin; Km, kanamycin.

Exo-muramidase NamZ of *B. subtilis*

pellet was resuspended in 50 μ l milliQ. Finally, 3 μ l of the bacterial supernatants was analyzed by HPLC-MS.

HPLC-MS analysis of supernatants, pNP-MurNAc, MurNAc-GlcNAc, and digested peptidoglycan

Sample analysis of digested peptidoglycan samples was accomplished using an electrospray ionisation-time of flight (ESI-TOF) mass spectrometer (MicroTOF II, Bruker Daltonics), operated in positive or negative ion mode, connected to an high-performance liquid chromatography (HPLC) system (UltiMate 3000, Dionex). For HPLC-MS analysis samples were injected (3 μ l for MurNAc-GlcNAc samples, MurNAc standard and for supernatants, 5 μ l for pNP-MurNAc and digested peptidoglycan samples) onto a Gemini C18 column (150 \times 4.6 mm, 5 μ m, 110 \AA , Phenomenex) and separated at 37 $^{\circ}\text{C}$ with a flow rate of 0.2 ml/min in accordance with a previously described program (35). The mass spectra of analyzed samples were displayed as extracted ion chromatograms (EIC) in DataAnalysis program (Bruker) and were presented in Prism 8 (GraphPad). The relative amounts of MurNAc from MurNAc standards and from release of MurNAc-GlcNAc substrate in enzyme kinetic studies were determined by calculating the area under the curve (AUC) of the corresponding EIC spectra for MurNAc.

Plasmid constructions for heterologous expression of namZ, amiE, cwIC, and atl^{Glc}

Genomic DNA of *B. subtilis* 168 and *S. aureus* USA300 JE2, serving as PCR templates, was prepared using GeneJET Genomic DNA Purification Kits. The genes *namZ*, *amiE*, and *cwIC* from *B. subtilis* 168 and *atl^{Glc}* from *S. aureus* USA300 JE2 were amplified by PCR using Phusion DNA polymerase using the primer pairs *ybbC_FW/ybbC_RV*, *RK-24/RK-20*, *AmiE_Bs_for/AmiE_Bs_rev* and *69_Atl_gluC_Fw/70_Atl_gluC_Rev*, respectively (listed in Table S2). In all cases the natural signal sequence was removed, allowing cytoplasmic expression in *E. coli*. Cloning and expression of *amiE* of *B. subtilis* along with *nagZ* have been achieved before (16). However, we decided to reclone *amiE* in a pET vector system for an easy, collective expression of all required enzymes in this study. PCR products and vectors were digested with the corresponding restriction enzymes, using *NdeI* and *XhoI* for *namZ* with pET29b, and *NcoI* and *XhoI* for *cwIC*, *atl^{Glc}* with pET28a, as well as for *amiE* with pET22b. Accordingly, using T4 DNA ligase *namZ* was ligated into a pET29b expression vector, *cwIC* and *atl^{Glc}* into pET28a expression vectors, and *amiE* into a pET22b expression vector (all vectors were from Novagen). Thereby all recombinant proteins were provided with a C-terminal His₆-tag. Chemically competent *E. coli* DH5 α cells were transformed with the ligation reaction mixtures. Recombinant plasmids pET29b-*namZ*, pET28a-*clwC*, pET28a-*atl^{Glc}*, and pET22b-*amiE* were isolated from kanamycin- or ampicillin-resistant *E. coli* cells and DNA sequences were verified by sequencing. Chemically competent *E. coli* BL21(DE3) cells were then transformed with pET29b-*namZ*,

pET28a-*clwC*, pET28a-*atl^{Glc}*, and pET22b-*amiE* and used to heterologously express the recombinant proteins under the control of the T7 promoter.

Expression and purification of recombinant NamZ, NagZ, AmiE, CwIC, and Atl^{Glc}

For the overexpression of NamZ and AmiE 2L LB medium and for overexpression of CwIC and Atl^{Glc} 1L LB medium, all supplemented with 50 μ g/ml kanamycin or 100 μ g/ml ampicillin (for pET22b-*amiE*) were inoculated with overnight cultures of *E. coli* BL21(DE3) harboring the expression plasmids pET29b-*namZ*, pET28a-*cwIC*, pET28a-*atl^{Glc}*, and pET22b-*amiE*. The cells were cultivated at 37 $^{\circ}\text{C}$ under continuous shaking. Expression of the recombinant proteins was induced at log phase (at OD₆₀₀ 0.7) by addition of IPTG at a final concentration of 1 mM. After induction the cells harboring pET29b-*namZ*, pET28a-*cwIC* and pET28a-*atl^{Glc}* were grown further for 3 h at 37 $^{\circ}\text{C}$, and the cells harboring pET22b-*amiE* were grown overnight at 18 $^{\circ}\text{C}$, all under continuous shaking. Cells were harvested by centrifugation at 4000g for 30 min at 4 $^{\circ}\text{C}$. Cell pellets were resuspended with 20 ml of sodium phosphate buffer A (20 mM Na₂HPO₄ * 2 H₂O, 500 mM NaCl, pH 7.5) each and disrupted by using French Press (Sim Aminco Spectronic Instruments, Inc) three times at 1000 psi. Cell debris and unbroken cells were removed by centrifugation at 38,000g for 60 min at 4 $^{\circ}\text{C}$. Purification of the C-terminally His₆-tagged proteins was performed by Ni²⁺ affinity chromatography. Therefore the obtained supernatants were filtered through 0.2 μ m filters (Sarstedt) and loaded on 1 ml His-Trap columns (GE Healthcare), pre-equilibrated with ten column volumes of each ddH₂O and sodium phosphate buffer A (20 mM Na₂HPO₄ * 2 H₂O, 500 mM NaCl, pH 7.5), using a protein purification system (ÄKTA purifier, GE Healthcare). Elution of the proteins was achieved by using a linear gradient of imidazole from 0 to 500 mM with sodium phosphate buffer B (20 mM Na₂HPO₄ * 2 H₂O, 500 mM NaCl, 500 mM imidazole, pH 7.5). Purity of the enzymes was analyzed by SDS-PAGE (12% polyacrylamide) stained with Coomassie Brilliant Blue G250. Peak fractions containing desired proteins were pooled and further purified by SEC (HiLoad 16/60 Superdex 200 column, GE Healthcare) using sodium phosphate buffer A as eluent. Peak fractions were analyzed for pure proteins by SDS-PAGE (12% polyacrylamide) and fractions containing pure enzymes were pooled. Protein concentrations were determined using the extinction coefficient at 280 nm (36,330 M⁻¹ cm⁻¹ for NamZ, 15,930 M⁻¹ cm⁻¹ for CwIC, 97,180 M⁻¹ cm⁻¹ for Atl^{Glc}, and 50,770 M⁻¹ cm⁻¹ for AmiE, ExpASy, ProtParam tool) and measured in a 1 ml quartz cuvette (Hellma) using a SpectraMax M2 spectrophotometer (Molecular Devices). NagZ was purified according to a previously published protocol (16).

Size-exclusion chromatography and multiangle light scattering (SEC-MALS)

Analytical SEC coupled to a multiangle light scattering apparatus (MALS, Wyatt Technology Corp) was used to

determine the apparent molecular masses of NamZ protein as described previously in (44). The experiments were done on a micro-Äkta chromatography system (GE Healthcare) connected to SEC Superose 6 Increase column (10/300 GL, GE Healthcare) at room temperature with a flow rate of 0.5 ml/min in sodium phosphate buffer A (20 mM Na₂HPO₄ * 2 H₂O, 500 mM NaCl, pH 7.5). MALS analysis was achieved by connecting micro-Äkta to a downstream MALS apparatus to which a refractometer (Optilab T-rEX, Wyatt Technology) and a miniDawn Treos system (Wyatt) were connected. The UV signals were plotted against the elution volume and the molar masses were calculated from the light scattering data using ASTRA 7 software (Wyatt) and the mass distribution was plotted over the eluted peaks.

Determination of the substrate specificity of recombinant NamZ with chromogenic substrates

NamZ activity was shown by cleavage of the chromogenic substrate para-nitrophenyl 2-acetamido-3-O-(D-1-carboxyethyl)-2-deoxy-β-D-glucopyranoside (pNP-MurNac). Specificity of NamZ was further examined by testing para-nitrophenyl 2-acetamido-2-deoxy-β-D-glucopyranoside (pNP-GlcNAc) (Sigma-Aldrich) and o-nitrophenyl β-D-galactopyranoside (oNP-Galactose) (Carl Roth GmbH + Co. KG) as substrates of NamZ. As positive control enzymes, NagZ (exo-β-N-acetylglucosaminidase of *B. subtilis*, purified according to (16)), and LacZ (β-D-galactosidase of *E. coli* (Hoffmann-La Roche) were used. In the test assay for NamZ specificity, a 100 μl reaction volume, containing chromogenic substrates (100 μM each) as listed above in 0.2 M sodium phosphate buffer (pH 8.0) was incubated for 30 min at 37 °C with purified enzymes (5 μg NamZ [0.7 μM], 5 μg NagZ [0.48 μM] and 10 μl LacZ [1500 U]). The reactions were initiated by addition of 10 μl of enzyme and stopped after 30 min by the addition of 100 μl borate buffer (0.5 M, pH 10.0). Specific release of the nitrophenol groups could be visualized by a yellow color and absorption was additionally measured at 405 nm. The assay was also conducted with pNP-isoMurNac, which however showed no yellow color release with none of the enzymes, including NamZ.

Determination of temperature and pH stability and optima of NamZ

Temperature stability of NamZ was determined by preincubating NamZ at different temperatures (*i.e.*, 4, 20, 37, 45, 55, and 60 °C) for 30 min and subsequently measuring the kinetics of the NamZ reaction under standard conditions (200 μM pNP-MurNac in 200 mM sodium phosphate buffer, pH 7.5 at 30 °C). Therefore, 10 μl each of the preincubated enzyme (500 ng) was added to 90 μl reaction mixtures containing 200 μM pNP-MurNac in 200 mM sodium phosphate buffer (pH 7.5), and the reaction at 37 °C was followed by measuring the absorption at 405 nm in a SpectraMax M2 microplate reader (Molecular Devices). Determination of temperature optimum of NamZ was achieved, by adding 10 μl of fresh enzyme (500 ng, 105 nM) to 90 μl reaction mixtures

containing 200 μM pNP-MurNac in 200 mM sodium phosphate buffer (pH 7.5) directly following the reaction at different temperatures (*i.e.*, 4, 20, 37, 45, 55, 60 °C) by measuring the absorption at 405 nm.

Determination of pH stability and pH optimum of NamZ was achieved, by applying buffers in the pH range of 2.0–10.0, *i.e.*, Clark and Lubs buffer (pH 2.0), citric acid-sodium phosphate buffer (pH 3.0–7.0), hydrochloric acid-Tris buffer (pH 8.0), and glycine-sodium hydroxide buffer (pH 9.0–10.0). For determination of pH stability, NamZ was diluted in appropriate buffers ranging from pH 2.0 to 10.0 at a final concentration of 50 ng/μl. The enzyme was preincubated for 30 min at ambient temperature (22 °C). After incubation the mixtures were buffer exchanged in centrifugal filter units (Amicon Ultra, 0.5 ml, 10 K, Merck Millipore) washed three times with 50 μl of sodium phosphate buffer (20 mM Na₂HPO₄, 500 mM NaCl, pH 7.5). After washing, the volume was brought up to 50 μl with 200 mM sodium phosphate buffer (pH 7.5) to maintain a final enzyme concentration of 50 ng/μl. The reaction assay was initiated by adding 10 μl of preincubated enzyme (500 ng, 105 nM) to a 90 μl reaction mixture under standard condition (as described above). For determination of pH optimum 90 μl reaction mixtures were prepared containing 200 μM pNP-MurNac in buffers of a particular pH in the range of 2.0–10.0. The reaction was initiated by adding 10 μl enzyme (500 ng, 105 nM) followed by incubation for 60 min at 37 °C; the reaction was stopped with borate buffer (250 mM disodium tetraborate, 1 M NaOH, pH 10.8). Samples were analyzed as described above.

Preparation of peptidoglycan

Peptidoglycan was required on the one hand to generate MurNac-GlcNAc as natural substrate for the biochemical characterization of NamZ and on the other hand to generate polymeric substrate for the sequential digest using NagZ, AmiE, and NamZ. Peptidoglycan of *B. subtilis* was prepared as previously described with slight modifications (45). For the production of MurNac-GlcNAc, two 5 L Erlenmeyer flasks each containing 1 L LB medium were inoculated with *B. subtilis* cells to yield an initial OD₆₀₀ of 0.1. The cells were cultured at 37 °C with continuous shaking at 120 rpm and harvested at an OD₆₀₀ of 1.8 by centrifugation at 5000g for 15 min at 4 °C. For the preparation of the peptidoglycan substrate for the sequential digest using NagZ, AmiE, and NamZ, exponential phase cells were harvested at an OD₆₀₀ of 1.0 by centrifugation at 5000g for 15 min at ambient temperature. For the preparation of MurNac-GlcNAc, the cells were washed with 25 ml PBS (137 mM NaCl, 2.7 mM KCl, 10 mM Na₂HPO₄, 1.8 mM KH₂PO₄) and the resulting pellets were stored at -20 °C. Frozen cells were suspended in 20 ml phosphate buffer (25 mM, pH 6.0) and added dropwise to a boiling solution (20 ml) of 8% SDS solution in phosphate buffer (25 mM, pH 6.0). After boiling under constant stirring for 30 min, the samples were cooled down to ambient temperature and centrifuged at 50,000g for 30 min at 40 °C. The pellet was washed with a phosphate buffer (25 mM, pH 6.0)

Exo-muramidase NamZ of *B. subtilis*

until the SDS in the sample was completely removed. The removal of SDS was proven with a methylene blue assay (46). The SDS-free pellet was suspended in 10 ml phosphate buffer (25 mM, pH 6.0) and incubated with 100 µg/ml α -amylase (from *Bacillus* sp., Sigma-Aldrich) for 1 h at 37 °C. Afterward, 200 µg/ml pronase (from *Streptomyces griseus*, Calbiochem, Merck KGaA) was added and the sample was incubated overnight at 37 °C. The next day, the sample was centrifuged at 16,500g for 10 min and the pellet was incubated with 5 ml of 1 M HCl for 4 h at 37 °C to remove the wall teichoic acids. After the HCl treatment, the pellet was washed with ddH₂O (16,500g, 10 min) until a pH of 5–6 was reached. The pellet was suspended in 20 ml phosphate buffer (25 mM, pH 6.0) and added dropwise into 20 ml of boiling phosphate buffer (25 mM, pH 6.0) and SDS (4%). Removal of SDS in the sample was performed as previously described.

For the peptidoglycan preparation for the sequential digests, the fresh cells were resuspended in 15 ml of Tris-HCl buffer (50 mM, pH 7.5) containing 20 µl proteinase K (20 mg/ml, NGS grade, 7BioScience GmbH) and added dropwise into 15 ml of boiling Tris-HCl buffer (50 mM, pH 7.5). After boiling for 60 min the sample was cooled down to room temperature and centrifuged at 2900g for 15 min at room temperature. The pellet was stored at –20 °C until the next day. Frozen pellet was resuspended in 6 ml Tris-HCl buffer containing MgSO₄ (50 mM, 10 mM MgSO₄, pH 7.5) and incubated together with 600 µg α -amylase (from *Bacillus* sp., Sigma-Aldrich), 10 µl RNase A (10 mg/ml, Thermo Fisher Scientific) and 10 µl DNase I (5 U/µl, Thermo Fisher Scientific) for 2 h at 37 °C under continuous shaking. After incubation, 20 µl proteinase K (20 mg/ml, NGS grade, 7BioScience GmbH) was added to the suspension and immediately added dropwise into boiling SDS solution (end-concentration of SDS was 2%), followed by boiling for 60 min. To remove the residual SDS, the sample was centrifuged in ultracentrifugation bottles (Beckman Coulter) at 104,500g at 40 °C for 30 min. The pellet was resuspended in prewarmed ddH₂O (about 60 °C) and centrifuged at least ten times in an ultracentrifuge (Beckman Coulter), until residual SDS was completely removed. To verify the removal of SDS from peptidoglycan samples, a methylene blue assay was performed (46). To remove wall teichoic acids, the peptidoglycan pellet was resuspended in 2 ml of 48% hydrofluoric acid (Sigma-Aldrich) and incubated for 48 h at 4 °C under vigorous shaking. Afterward, the sample was washed several times with phosphate buffer (100 mM, pH 7.0, 20,000g, 5 min) and the peptidoglycan pellet was neutralized with ddH₂O until the pH of the supernatant was above 6.5. Finally, the purified peptidoglycan was dried (SpeedVac, Christ, RVC2-18) and weighed.

Purification of MurNAc-GlcNAc

To generate MurNAc-GlcNAc, 900 mg peptidoglycan was incubated with CwIC and AtI^{Glc} (each 1 µM) in 90 ml sodium phosphate buffer (100 mM, pH 8.0) overnight at 37 °C under continuous shaking. Afterward, the reaction mixture was heated to 95 °C for 25 min. In total, 90 µl of the heat-treated

samples was loaded on a semipreparative Gemini C18 column (250 × 10 mm, 110 Å, 5 µm, Phenomenex) and separated *via* reversed-phase HPLC (VWR Hitachi Chromaster) at 20 °C with a flow rate of 1.5 ml/min in accordance with a previously described program (35) with slight modifications, starting with 10 min of washing with 100% buffer A (0.1% formic acid, 0.05% ammonium formate in water), afterward injection of the sample and another 5 min washing step with 100% buffer A. A linear gradient to 40% buffer B (acetonitrile) over 30 min was followed by a 5 min hold at 40% buffer B. Re-equilibration within a 1 min step to 100% buffer A was followed by a 10 min wash step at 100% buffer A. Fractions were collected in 1.5 ml volumes, representing 1 min of flow each. Collected fractions containing MurNAc-GlcNAc were lyophilized, suspended in 3 ml ddH₂O, aliquoted in tubes, and dried at 40 °C using SpeedVac (Christ, RVC2-18).

Specificity of NamZ was determined using natural cell wall disaccharides MurNAc-GlcNAc (as prepared above) and GlcNAc-MurNAc (Carbosynth Ltd). For each substrate, two 25 µl reaction mixtures were prepared containing either 100 µM MurNAc-GlcNAc or 100 µM GlcNAc-MurNAc in 0.2 M sodium phosphate buffer (pH 7.0). The reactions were initiated by adding 500 ng purified NamZ (420 nM). In addition, NagZ (500 ng, 280 nM) was added as a control to the reaction mixtures. As a negative control, reaction mixtures without added enzymes were incubated. The reaction mixtures were incubated at 37 °C for 30 min and stopped with a buffer containing 1% formic acid and 0.5% ammonium formate in water (pH 3.2). The reaction mixture was transferred into vials and analyzed directly by HPLC-MS under conditions as described above.

Determination of enzyme kinetic parameters for pNP-MurNAc and MurNAc-GlcNAc substrates

Determination of kinetic parameters of NamZ was achieved by using both the chemically synthesized substrate pNP-MurNAc and the purified substrate MurNAc-GlcNAc. Before starting the kinetic experiments, the purity of pNP-MurNAc was checked by HPLC-MS analysis. For pNP-MurNAc, 100 µM substrate in phosphate buffer (0.2 M, pH 7.0) was analyzed and compared with the same reaction mixture containing additionally 500 ng NamZ (105 nM). Both mixtures were incubated at 37 °C for 30 min and subsequently analyzed using HPLC-MS. Since we discovered that the pNP-MurNAc stock in MeOH formed traces of methyl ester, which could not serve as a substrate for NamZ, we chose incubation under basic conditions to fully hydrolyze the ester traces of pNP-MurNAc. Therefore, 1 mM pNP-MurNAc was preincubated in phosphate buffer (20 mM, pH 8.0) at 37 °C for 30 min. Afterward, 100 µM preincubated pNP-MurNAc in phosphate buffer (0.2 M, pH 7.0) was analyzed and compared with the same reaction mixture containing additionally 500 ng NamZ (420 nM). Both mixtures were, again, incubated at 37 °C for 30 min and subsequently analyzed using HPLC-MS.

To ascertain the kinetic parameters for pNP-MurNAc, different concentrations of pNP-MurNAc in 0.2 M

phosphate buffer (pH 8.0) were used, after preincubation in phosphate buffer as described above. In a 96-well plate (Greiner), a 90 μ l reaction mixture containing pNP-MurNAc ranging from 13 to 860 μ M in phosphate buffer (0.2 M, pH 8.0) was incubated at 37 °C. The reaction was started by addition of 10 μ l enzyme (500 ng, 105 nM). The reaction was continuously monitored at 37 °C for 30 min at 405 nm with a Spark 10 M microplate reader (Tecan). To determine the amount of released 4-nitrophenol by the action of NamZ on pNP-MurNAc, a 4-nitrophenol standard (Sigma Aldrich) dissolved in phosphate buffer (0.2 M, pH 8.0) with concentrations from 13 to 430 μ M was also prepared for measurement at 405 nm with the same microplate reader as mentioned above. The experimental data of the enzyme kinetics were evaluated by nonlinear regression of the reaction curve using the program Prism 6 (GraphPad).

To determine the kinetic parameters for MurNAc-GlcNAc, different concentrations of MurNAc-GlcNAc in 0.2 M phosphate buffer (pH 7.0) were used. In eppendorf tubes (Sarstedt), a 18 μ l reaction mixture containing MurNAc-GlcNAc ranging from 0.025 to 6 mM in phosphate buffer (0.2 M, pH 7.0) was incubated at 37 °C. The reaction was started by adding 2 μ l enzyme (10 ng, 10.5 nM). The reaction mixture was incubated at 37 °C for 5 min and stopped with 20 μ l of stopping buffer containing 1% formic acid and 0.5% ammonium formate in water (pH 3.2). The reaction mixture was transferred into vials and analyzed by HPLC-MS. To determine the amount of released MurNAc by the action of NamZ on MurNAc-GlcNAc, a MurNAc standard with concentrations from 0.0063 to 0.8 mM was also prepared for HPLC-MS analysis. To ensure the same ionization conditions for the standard and the reaction mixture, the standard was dissolved in an equal mixture of 0.2 M phosphate buffer (pH 7.0) and the stopping buffer.

Sequential digest with NagZ, AmiE, and NamZ

To perform the sequential digest, 2.5 mg of purified *B. subtilis* peptidoglycan was dissolved in 100 μ l phosphate buffer (0.2 M, pH 7.0). To the dissolved peptidoglycan a 50 μ l mixture containing 2.5 μ M NagZ (26.7 μ g), 2.5 μ M AmiE (17.9 μ g), and 2.5 μ M NamZ (19.5 μ g) in phosphate buffer (0.2 M, pH 7.0) was added, resulting in a total volume of 150 μ l. The digest was incubated overnight at 37 °C under continuous shaking. After incubation the reaction was stopped by heating at 95 °C for 30 min. To separate cell wall monosaccharides and peptides from undigested peptidoglycan, the reaction mixture was centrifuged at 12,100g for 15 min and the supernatant was dried at 37 °C (SpeedVac Christ, RVC2-18). Afterward, the pellets were dissolved in 50 μ l ddH₂O and transferred into vials to be analyzed using HPLC-MS.

Taxonomic distribution of NamZ and other recycling enzymes

A taxonomic tree was constructed that depicts the distribution of homologs of the recycling proteins NamZ and NagZ of *B. subtilis* 168, as well as other recycling proteins, MurQ of *E. coli* K12, MupG of *S. aureus* USA300, and AmgK, MupP, and

MurU of *P. putida* KT2440. The occurrence of the homologs was investigated in organisms included on the representative NCBI RefSeq genomes. The protein sequences for NagZ (P40406) and NamZ (P40407), as well as MurQ (P76535), MupG (A0A0H2XHV5), AmgK (Q88QT3), MupP (Q88M11), and MurU (Q88QT2), obtained from UniProt and BLAST searches were analyzed using the MultiGeneBlast application (47). MultiGeneBlast allows homology searches with more than one input sequence and also displays the localization of genes coding for possible homologues in the genome. The application was run in "architecture search" mode to find the genes coding for possible homologues within a distance of 20 kb, regardless of their colocalization or order of occurrence on the genome. Furthermore, thresholds were set for a minimum sequence coverage of 50% and a minimum identity of 20%, leaving the other settings at the default values. Matches found were annotated and visualized in a tree constructed according to the NCBI taxonomy using the iTOL v3 web service (48).

Data availability

All data generated and analyzed during this study are contained within the article and the [supporting information](#). The structural modeling data are available from the corresponding author on reasonable request.

Supporting information—This article contains [supporting information](#).

Acknowledgments—This work was further supported by the DFG-funded Cluster of Excellence EXC 2124 Controlling Microbes to Fight Infections. We thank Amanda Duckworth for the construction of plasmid pET29b-namZ and Libera lo Presti for manuscript editing.

Author contributions—C. M.: conceptualization; M. M., M. C., I. H., K. A. S., Q. X., and M. B.: data curation; M. M., R. M. K., T. T., and M. B.: formal analysis; C. M.: funding acquisition; M. M. and C. M.: investigation; M. M., R. M. K., and C. M.: methodology; C. M.: project administration; M. M., M. C., R. M. K., T. T., K. B., A. E., Q. X., and M. B.: resources; M. B., A. T., and C. M.: supervision; M. M., M. C., A. T., and M. B.: validation; M. M., M. B., and C. M.: visualization; M. M. and C. M.: writing - original draft; M. B., A. T. and C. M.: writing - review and editing.

Funding and additional information—C. M. acknowledges funding by the Ministry of Science, Research and Art of the state Baden-Württemberg (programme glycobiology/glycobiotechnology) and by the Deutsche Forschungsgemeinschaft (DFG, German Research Foundation), grants SFB766, Project-ID 398967434–TRR 261, and Project-ID 174858087–GRK1708.

Conflict of interest—The authors declare that they have no conflicts of interest with the content of this article.

Abbreviations—The abbreviations used are: AUC, area under curve; BPC, base peak chromatogram; EIC, extracted ion chromatogram; GlcNAc, *N*-acetylglucosamine; MurNAc, *N*-acetylmuramic acid; pNP-GlcNAc, para-nitrophenyl 2-acetamido-2-deoxy- β -D-

Exo-muramidase NamZ of *B. subtilis*

glucopyranoside; pNP-MurNAc, para-nitrophenyl 2-acetamido-3-O-(D-1-carboxyethyl)-2-deoxy-β-D-glucopyranoside.

References

- Warren, R. A. (1996) Microbial hydrolysis of polysaccharides. *Annu. Rev. Microbiol.* **50**, 183–212
- Jalak, J., Kurasin, M., Teugias, H., and Valjamae, P. (2012) Endo-exo synergism in cellulose hydrolysis revisited. *J. Biol. Chem.* **287**, 28802–28815
- Wang, J., Quirk, A., Lipkowsky, J., Dutcher, J. R., and Clarke, A. J. (2013) Direct *in situ* observation of synergism between cellulolytic enzymes during the biodegradation of crystalline cellulose fibers. *Langmuir* **29**, 14997–15005
- Itoh, T., and Kimoto, H. (2019) Bacterial chitinase system as a model of chitin biodegradation. *Adv. Exp. Med. Biol.* **1142**, 131–151
- Walter, A., and Mayer, C. (2019) Peptidoglycan structure, biosynthesis, and dynamics during bacterial growth. In: Cohen, E., Merzendorfer, H., eds. *Extracellular Sugar-Base Biopolymers Matrices*, Elsevier, Amsterdam, Netherlands: 237–299
- Strynadka, N. C., and James, M. N. (1996) Lysozyme: A model enzyme in protein crystallography. *Exs* **75**, 185–222
- Ragland, S. A., and Criss, A. K. (2017) From bacterial killing to immune modulation: Recent insights into the functions of lysozyme. *PLoS Pathog.* **13**, e1006512
- Litzinger, S., Fischer, S., Polzer, P., Diederichs, K., Welte, W., and Mayer, C. (2010) Structural and kinetic analysis of *Bacillus subtilis* N-acetylglucosaminidase reveals a unique Asp-His dyad mechanism. *J. Biol. Chem.* **285**, 35675–35684
- Reith, J., and Mayer, C. (2011) Peptidoglycan turnover and recycling in Gram-positive bacteria. *Appl. Microbiol. Biotechnol.* **92**, 1–11
- Mayer, C., Kluj, R. M., Muhleck, M., Walter, A., Unsleber, S., Hottmann, I., and Borisova, M. (2019) Bacteria's different ways to recycle their own cell wall. *Int. J. Med. Microbiol.* **309**, 151326
- Scheurwater, E., Reid, C. W., and Clarke, A. J. (2008) Lytic transglycosylases: Bacterial space-making autolysins. *Int. J. Biochem. Cell Biol.* **40**, 586–591
- Lee, M., Heseck, D., Llarrull, L. I., Lastochkin, E., Pi, H., Boggess, B., and Mobashery, S. (2013) Reactions of all *Escherichia coli* lytic transglycosylases with bacterial cell wall. *J. Am. Chem. Soc.* **135**, 3311–3314
- Sugai, M., Komatsuzawa, H., Akiyama, T., Hong, Y. M., Oshida, T., Miyake, Y., Yamaguchi, T., and Suganaka, H. (1995) Identification of endo-beta-N-acetylglucosaminidase and N-acetylmuramyl-L-alanine amidase as cluster-dispersing enzymes in *Staphylococcus aureus*. *J. Bacteriol.* **177**, 1491–1496
- Wheeler, R., Turner, R. D., Bailey, R. G., Salamaga, B., Mesnage, S., Mohamad, S. A., Hayhurst, E. J., Horsburgh, M., Hobbs, J. K., and Foster, S. J. (2015) Bacterial cell enlargement requires control of cell wall stiffness mediated by peptidoglycan hydrolases. *mBio* **6**, e00660
- Kluj, R. M., Ebner, P., Adamek, M., Ziemert, N., Mayer, C., and Borisova, M. (2018) Recovery of the peptidoglycan turnover product released by the autolysin Atl in *Staphylococcus aureus* involves the phosphotransferase system transporter MurP and the novel 6-phospho-N-acetylmuramidase MupG. *Front. Microbiol.* **9**, 2725
- Litzinger, S., Duckworth, A., Nitzsche, K., Risinger, C., Wittmann, V., and Mayer, C. (2010) Muropeptide rescue in *Bacillus subtilis* involves sequential hydrolysis by β-N-acetylglucosaminidase and N-acetylmuramyl-L-alanine amidase. *J. Bacteriol.* **192**, 3132–3143
- Bacik, J. P., Whitworth, G. E., Stubbs, K. A., Vocadlo, D. J., and Mark, B. L. (2012) Active site plasticity within the glycoside hydrolase NagZ underlies a dynamic mechanism of substrate distortion. *Chem. Biol.* **19**, 1471–1482
- Acebron, I., Mahasenan, K. V., De Benedetti, S., Lee, M., Artola-Recolons, C., Heseck, D., Wang, H., Hermoso, J. A., and Mobashery, S. (2017) Catalytic cycle of the N-acetylglucosaminidase NagZ from *Pseudomonas aeruginosa*. *J. Am. Chem. Soc.* **139**, 6795–6798
- del Rio, L. A., Berkeley, R. C. W., Brewer, S. J., and Roberts, S. E. (1973) An enzyme from *Bacillus subtilis* B with exo-β-N-acetylmuramidase activity. *FEBS Lett.* **37**, 7–9
- del Rio, L. A., and Berkeley, R. C. W. (1976) Exo-β-N-acetylmuramidase — novel hexosaminidase. Production by *Bacillus subtilis* B, purification and characterization. *Eur. J. Biochem.* **65**, 3–12
- Borisova, M., Gaupp, R., Duckworth, A., Schneider, A., Dalugge, D., Mühleck, M., Deubel, D., Unsleber, S., Yu, W., Muth, G., Bischoff, M., Götz, F., and Mayer, C. (2016) Peptidoglycan recycling in gram-positive bacteria is crucial for survival in stationary phase. *mBio* **7**, e00923-00916
- Jaeger, T., Arsic, M., and Mayer, C. (2005) Scission of the lactyl ether bond of N-acetylmuramic acid by *Escherichia coli* “etherase”. *J. Biol. Chem.* **280**, 30100–30106
- Jaeger, T., and Mayer, C. (2008) The transcriptional factors MurR and catabolite activator protein regulate N-acetylmuramic acid catabolism in *Escherichia coli*. *J. Bacteriol.* **190**, 6598–6608
- Dahl, U., Jaeger, T., Nguyen, B. T., Sattler, J. M., and Mayer, C. (2004) Identification of a phosphotransferase system of *Escherichia coli* required for growth on N-acetylmuramic acid. *J. Bacteriol.* **186**, 2385–2392
- Nicolas, P., Mader, U., Dervyn, E., Rochat, T., Leduc, A., Pigeonneau, N., Bidnenko, E., Marchadier, E., Hoebeke, M., Aymerich, S., Becher, D., Bisicchia, P., Botella, E., Delumeau, O., Doherty, G., et al. (2012) Condition-dependent transcriptome reveals high-level regulatory architecture in *Bacillus subtilis*. *Science* **335**, 1103–1106
- Almagro Armenteros, J. J., Tsirigos, K. D., Sonderby, C. K., Petersen, T. N., Winther, O., Brunak, S., von Heijne, G., and Nielsen, H. (2019) SignalP 5.0 improves signal peptide predictions using deep neural networks. *Nat. Biotechnol.* **37**, 420–423
- Koo, B. M., Kritikos, G., Farelli, J. D., Todor, H., Tong, K., Kimsey, H., Wapinski, I., Galardini, M., Cabal, A., Peters, J. M., Hachmann, A. B., Rudner, D. Z., Allen, K. N., Typas, A., and Gross, C. A. (2017) Construction and analysis of two genome-scale deletion libraries for *Bacillus subtilis*. *Cell Syst.* **4**, 291–305.e297
- Miller, J. H. (1972) An assay for beta-galactosidase *Experiments in Molecular Genetics*, 1972 Ed., Cold Spring Harbor Laboratory Press, Cold Spring Harbor, NY: 352–355
- Ortiz, J. M., Gillespie, J. B., and Berkeley, R. C. (1972) An exo-β-N-acetylglucosaminidase from *Bacillus subtilis* B; extraction and purification. *Biochim. Biophys. Acta* **289**, 174–186
- Berkeley, R. C., Brewer, S. J., Ortiz, J. M., and Gillespie, J. B. (1973) An exo-b-N-acetylglucosaminidase from *Bacillus subtilis* B; characterization. *Biochim. Biophys. Acta* **309**, 157–168
- del Rio, L. A., and Berkeley, R. C. W. (1975) A substrate for the fluorogenic assay of exo-β-N-acetylmuramidase: Synthesis and purification of 4-methylumbelliferyl N-acetylmuramide. *Anal. Biochem.* **66**, 405–411
- Jeanloz, R. W., Walker, E., and Sinay, P. (1968) Synthesis of various glycosides of 2-amino-3-O-(D-1-carboxyethyl)-2-deoxy-D-glucopyranose (muramic acid). *Carbohydr. Res.* **6**, 184–196
- Walter, A., Friz, S., and Mayer, C. (2021) Chitin, chitin oligosaccharide and chitin disaccharide metabolism of *Escherichia coli* revisited: Reassignment of the roles of ChiA, ChbR, ChbF and ChbG. *Microb. Physiol.* in press
- Hildebrand, A., Remmert, M., Biegert, A., and Soding, J. (2009) Fast and accurate automatic structure prediction with HHpred. *Proteins* **77** Suppl **9**, 128–132
- Gisin, J., Schneider, A., Nägele, B., Borisova, M., and Mayer, C. (2013) A cell wall recycling shortcut that bypasses peptidoglycan *de novo* biosynthesis. *Nat. Chem. Biol.* **9**, 491–493
- Sudiarta, I. P., Fukushima, T., and Sekiguchi, J. (2010) *Bacillus subtilis* CwlQ (previous YjbJ) is a bifunctional enzyme exhibiting muramidase and soluble-lytic transglycosylase activities. *Biochem. Biophys. Res. Commun.* **398**, 606–612
- Horsburgh, G. J., Atrih, A., Williamson, M. P., and Foster, S. J. (2003) LytG of *Bacillus subtilis* is a novel peptidoglycan hydrolase: The major active glucosaminidase. *Biochemistry* **42**, 257–264
- Rajan, S. S., Yang, X., Collart, F., Yip, V. L., Withers, S. G., Varrot, A., Thompson, J., Davies, G. J., and Anderson, W. F. (2004) Novel catalytic mechanism of glycoside hydrolysis based on the structure of an NAD⁺

- Mn²⁺-dependent phospho- α -glucosidase from *Bacillus subtilis*. *Structure (Camb)* **12**, 1619–1629
39. Yip, V. L., Varrot, A., Davies, G. J., Rajan, S. S., Yang, X., Thompson, J., Anderson, W. F., and Withers, S. G. (2004) An unusual mechanism of glycoside hydrolysis involving redox and elimination steps by a family 4 beta-glycosidase from *Thermotoga maritima*. *J. Am. Chem. Soc.* **126**, 8354–8355
 40. Yip, V. L., Thompson, J., and Withers, S. G. (2007) Mechanism of GlvA from *Bacillus subtilis*: A detailed kinetic analysis of a 6-phospho- α -glucosidase from glycoside hydrolase family 4. *Biochemistry* **46**, 9840–9852
 41. Liu, Q. P., Sulzenbacher, G., Yuan, H., Bennett, E. P., Pietz, G., Saunders, K., Spence, J., Nudelman, E., Levery, S. B., White, T., Neveu, J. M., Lane, W. S., Bourne, Y., Olsson, M. L., Henrissat, B., *et al.* (2007) Bacterial glycosidases for the production of universal red blood cells. *Nat. Biotechnol.* **25**, 454–464
 42. Laurino, P., Toth-Petroczy, A., Meana-Paneda, R., Lin, W., Truhlar, D. G., and Tawfik, D. S. (2016) An ancient fingerprint indicates the common ancestry of Rossmann-fold enzymes utilizing different ribose-based co-factors. *PLoS Biol.* **14**, e1002396
 43. Msadek, T., Kunst, F., Henner, D., Klier, A., Rapoport, G., and Dedonder, R. (1990) Signal transduction pathway controlling synthesis of a class of degradative enzymes in *Bacillus subtilis*: Expression of the regulatory genes and analysis of mutations in *degS* and *degU*. *J. Bacteriol.* **172**, 824–834
 44. Selim, K. A., Lapina, T., Forchhammer, K., and Ermilova, E. (2020) Interaction of *N*-acetyl-L-glutamate kinase with the PII signal transducer in the non-photosynthetic alga *Polytomella parva*: Co-evolution towards a hetero-oligomeric enzyme. *FEBS J.* **287**, 465–482
 45. Schaub, R. E., and Dillard, J. P. (2017) Digestion of peptidoglycan and analysis of soluble fragments. *Bio Protoc.* **7**, e2438
 46. Hayashi, K. (1975) A rapid determination of sodium dodecyl sulfate with methylene blue. *Anal. Biochem.* **67**, 503–506
 47. Medema, M. H., Takano, E., and Breitling, R. (2013) Detecting sequence homology at the gene cluster level with MultiGeneBlast. *Mol. Biol. Evol.* **30**, 1218–1223
 48. Letunic, I., and Bork, P. (2016) Interactive tree of life (iTOL) v3: An online tool for the display and annotation of phylogenetic and other trees. *Nucleic Acids Res.* **44**, W242–W245
 49. Fey, P. D., Endres, J. L., Yajjala, V. K., Widhelm, T. J., Boissy, R. J., Bose, J. L., and Bayles, K. W. (2013) A genetic resource for rapid and comprehensive phenotype screening of nonessential *Staphylococcus aureus* genes. *mBio* **4**, e00537-00512
 50. Fumeaux, C., and Bernhardt, T. G. (2017) Identification of MupP as a new peptidoglycan recycling factor and antibiotic resistance determinant in *Pseudomonas aeruginosa*. *mBio* **8**, e00102-17